Sliding Mode Controller for Single Phase Grid Connected Voltage Source Inverter with LCL Filter

Ahmad Khodor AL Ahmad

Submitted to the
Institute of Graduate Studies and Research
in partial fulfillment of the requirements for the degree of

Master of Science
in
Electrical and Electronic Engineering

Eastern Mediterranean University
February 2017
Gazimağusa, North Cyprus

Approval of the Institute of Graduate Studies and Research

Prof. Dr. Mustafa Tümer
Director

I certify that this thesis satisfies the requirements as a thesis for the degree of Master of Science in Electrical and Electronic Engineering

Prof. Dr. Hasan Demirel
Chair, Department of
Electrical and Electronic Engineering

We certify that we have read this thesis and that in our opinion it is fully adequate in scope and quality as a thesis for the degree of Master of applied science in electrical and electronic engineering.

Prof. Dr. Osman Kükrer
Supervisor

Examining committee

1. Prof. Dr. Hasan Amca _____

2. Prof. Dr. Hasan Kömürcügil _____

3. Prof. Dr. Osman Kükrer _____

4. Prof. Dr. Şener Uysal _____

ABSTRACT

Many researchers have focused widely on suppressing the steady state sinusoidal tracking error and the total harmonic distortion in grid-connected inverter systems. In this thesis, a sliding mode control strategy with integral and mutli-resonant controllers is used to control a single phase voltage source grid connected inverter. This method leads to a sliding surface where all the states of the system remain on and sliding until reaching the equilibrium point which is the origin in the steady state. Integral term for grid current error is added to suppress the magnitude of the error in grid current but the results show that this term has no effect on the harmonic distortion of the system especially when an external disturbance is applied to the system from the grid voltage. So, another term called multi-resonant is added. This multi-resonant term is able to suppress the magnitude of the disturbance and the total harmonic distortion in the system.

Simulation results for single-phase grid-connected inverter is shown using Simulink (matlab 2015) to prove the effectiveness of the proposed control strategy. These results are compared with the results in [11] where the tracking precision of the grid current is improved from 0.91% to 0.17% and the THD of the grid current from 0.76% to 0.05%.

Keyword: Voltage source inverter (VSI), LCL filter, Sliding mode control (SMC), Integral controller, Multi-resonant controller, Grid current tracking error, Total Harmonic Distortion (THD).

ÖZ

Birçok araştırmacı, şebekeye bağlı evirgeç sistemlerindeki akımların durağan durumdaki takip hatasını ve toplam harmonik bozunumunu azaltmaya yoğunlaşmıştır. Bu tezde, şebekeye bağlı voltaj kaynaklı tek faz bir evirgeçin denetimi için integral ve çoklu-rezonant denetleyiciler kullanan bir kayan kipli bir denetim yöntem kullanılmıştır. Bu yöntem, dizge durum değişkenlerinin üzerinde olduğu ve kayarak, dizgenin durağan durumdaki denge noktasına ulaştığı bir kayma yüzeyi yaratmaktadır. Denetleyiciye, şebeke akımındaki hatanın büyüklüğünü gidermek için akım hatasını kullanan bir integral terim eklenmiştir. Fakat sonuçlar bu terimin, özellikle şebeke voltajindan kaynaklanan bir dış bozucu etki uygulandığında sistemin harmonik bozunumuna fazla etki etmediğini göstermektedir. Dolayısiyle, denetleyiciye çoklu-rezonantlı bir terim eklenmiştir. Bu terim dış bozucunun etkisini ve akımdaki harmonik bozunumu giderdiği görülmüştür.

Şebekeye bağlı evirgeçin önerilen denetim yöntemi ile çalıştırılmasının benzetim sonuçları Simulink (Matlab) kullanılarak elde edilmiş, ve yöntemin gücü bu yolla kanıtlanmıştır. Bu sonuçlar, [11] verilenlerle karşılaştırılmış, ve bunlara göre takip etme hatasında %0.91 den %0.17 ye, THD de ise %0.76 dan %0.03 e iyileştirme sağlandığı görülmüştür.

Anahtar sözcükler: Voltaj kaynaklı evirgeç, LCL süzgeç, Kayan kipli denetim, İntegral denetim, Çoklu-rezonant denetim, Şebeke akımı takip hatası, Toplam harmonik bozunum.

To:

My Beloved Family

ACKNOWLEDGMENT

I would like to thank my supervisor, Prof. Dr. OSMAN KÜKRER, for his encouragement and support during my master degree's period. I gratefully acknowledge the invaluable guidance and advise he has provided me throughout this process. I appreciate the opportunities he has given me and cannot say enough about my gratitude to him.

I would like to thank the Chairman of the Electrical and Electronic Department Prof. Dr. Hasan Demirel for his advice, support and friendship. His support has been invaluable on both academic and personal level, for which I am very grateful.

Special thanks also go to all my friends and especially my dear friend Assist. Hamza Makhamreh for sharing the literature and providing invaluable assistance.

Last but not least, I would like to express my deepest gratitude to my lovely family; they gave me a chance for completing my higher education in Cyprus. Without their support, both in financial and emotional matter, achievement of this level was impossible.

TABLE OF CONTENTS

ABSTRACT……iii

ÖZ……iv

ACKNOWLEDGEMENT……...vi

LIST OF TABLES……..vii

LIST OF FIGURES……..x

LIST OF SYMBOLS…….....xv

LIST OF ABBREVIATIONS……xviii

1 INTRODUCTION …...…….……1

1.1 Inverter ……..…….…….....…..…..……2

1.1.1 Single phase half bridge inverter ……..……....……4

1.1.2. Single phase full bridge inverter …….…..……..……..……4

1.1.3 Three phase inverter……...……5

1.1.4 Pulse width modulation PWM ……..7

1.2 Thesis contribution…….……..7

2 Grid connected voltage source inverter with LCL filter…...……...……..…9

2.1 System Definition...……..……9

2.1.1 Reference functions …….……...……11

2.1.2 Steady state errors …….....…..12

2.1.3 Uncertainty parameters ……...……12

2.1.4 Control input …….……..13

2.2 Representing the system in state space model …….…….…13

3 SLIDING MODE CONTROL STRATEGY……...17

3.1 Theory of operating for Sliding mode control ……..……..……..17

3.1.1 Control input determination ……..……..……..……18

4 THE CONTROLLERS OF THE SYSTEM ……...……22

4.1 The Operated Controllers in the system……...….……22

4.1.1 Sliding mode controller ……..……..…..22

4.1.2 Addition of Integral controller ……..…….25

4.1.3 Addition of multi-resonant terms……..……...…….……..…..…..25

4.2 Theoretical results ……...……26

4.2.1 SMC alone ……..….…….27

4.2.2 SMC and IC ……...…...29

4.2.3 SMC, IC, and MRC ……...…...30

5 THE PROPOSED MODEL AND SIMULATION RESULTS……...……31

5.1 The proposed Model for the whole system ……..…...….….31

5.2 Simulation results…….…...…..….38

5.2.1 SMC alone ……..……39

5.2.2 SMC and MRC ……..……..……...44

5.2.3 SMC and IC ……...…...……..46

5.2.4 All controllers (SMC, IC, MRC) …….…….....47

5.3 Comparison between this thesis and the IEEE transaction paper in [11]…….49

6 CONCLUSION AND FUTURE WORK……51

6.1 Conclusion…….51

6.2 Future work……52

REFERENCES ……..…..53

APPENDICES ……..……..55

Appendix A: Matlab code - Steady state Mode ……..…..…….…56

LIST OF TABLES

Table 1: The values of the system parameters……..……..27

Table 2: Similarities in the parameters of the model used in this thesis and the other one in the IEEE transaction paper in [11]…….....……49

Table 3: Differences in the parameters of the model used in this thesis and the other one in the IEEE transaction paper in [11] ……...…….…..…50

Table 4: Comparison in the magnitude of error and THD in four different controllers in this thesis with that in the IEEE transaction paper in [11]……...…...50

LIST OF FIGURES

Fig 1: Circuit diagram of an inverter with LC filter connected to the load……2

Fig 2: Circuit diagram of voltage source inverter with LC filter connected to the load……..……..2

Fig 3: Circuit diagram of current source inverter with L filter connected to the load……2

Fig 4: Circuit diagram of voltage source inverter with LC filter connected to the load with variable DC supply at its input terminal……..…..……3

Fig 5: Variable square wave form for the inverter output voltage according to variable input DC supply…….……..……...3

Fig 6: Circuit diagram of voltage source inverter with fixed DC supply at its input terminal…….……4

Fig 7: Circuit diagram of single phase half bridge voltage source inverter with fixed DC supply at its input terminal and the wave form of its output voltage…….…...4

Fig 8: Circuit diagram of single phase full bridge voltage source inverter with fixed DC supply at its input terminal and the wave form of its output voltage……..…5

Fig 9: Circuit diagram of three phase voltage source inverter with fixed DC supply at its input terminal……..…….6

Fig 10: Output voltage wave forms of three phase voltage source inverter with fixed DC supply at its input terminal……...…….……6

Fig 11: Method of operation of PWM technique……..……7

Fig 12: voltage source grid connected inverter with LCL filter 10

Figure 13: Theory of operation of sliding mode control ……..…..18

Figure 14: Grid current error for c_3=1 as function of time using SMC alone…….…27

Figure 15: Grid current error for c_3=30 as function of time using SMC alone……...27

Figure 16: Grid current error for c_3=40 as function of time using SMC alone……...28

Figure 17: Grid current error for c_3=50 as function of time using SMC alone…...…28

Figure 18: Grid current error for c_3=40 and Ki=10^3 as function of time using SMC and integral controller …….……..…….29

Figure 19: Grid current error for c_3=40 and Ki=10^4 as function of time using SMC and integral controller……..……..…….....29

Figure 20: Grid current error for c_3=40 and Ki=5*10^4 as function of time using SMC and integral controller…….……..……..29

Figure 21: Grid current error for c_3=40, Ki=10^4, and Kr=30 as function of time using sliding mode controller, integral controller, and Multi-resonant controllers…....….30

Figure 22: Control diagram for single phase inverter with LCL filter using SMC, IC, and MRC……..……...31

Figure 23: The proposed model for the whole system……33

Figure 24: A model that describes the references in the system that are defined in Chapter 1……...…….…….34

Figure 25: A model that describes the errors in system that are defined in Chapter 1 …….34

Figure 26: A model that describes the switching function in system that is defined in Chapter 2……...…….…….34

Figure 27: A model that describes the integral controller in system that is defined in Chapter 3……...…….35

Figure 28: A model that describes the multi-resonant controller in system that is defined in Chapter 3 ……...……...…….35

Figure 29: A model that describes the switching function after combining of all controllers include SMC, IC, and MRC as defined in Chapter 3…….....35

Figure 30: A model that describes the linear and non-linear parts of the control input as defined in Chapter 2 …….……..……...36

Figure 31: A model that describes the control input at steady state as defined in Chapter 1…….…….……...…….....….36

Figure 32: A model that describes the equivalent part of the control input as defined in Chapter 2 ……..……...……...37

Figure 33: Total control input for the system as defined in chapter 3……...37

Figure 34: Pulse width modulation technique that is responsible for generating pulses to the switches of the inverter……...……..38

Figure 35: Grid current error as function of time in case of SMC for c_3=40 with applied disturbance by decreasing the grid reference current from 35A to 25A. 39

Figure 36: Grid current error as function of time in case SMC with applied disturbance by decreasing the grid reference current from 35A to 25A after zooming the previous Figure. ……..…….39

Figure 37: Grid current and grid voltage as function of time in case SMC with applied disturbance by decreasing the grid reference current from 35A to 25A …...39

Figure 38: Inverter output voltage as function of time using SMC controller alone..40

Figure 39: Control input of the system as function of time using SMC…….40

Figure 40: Grid current error as function of time in case SMC for c_3=40 with inserting 3^{rd} and 5^{th} harmonics in grid voltage at t=0.176sec.……....…….41

Figure 41: Grid current error as function of time in case SMC for c_3=40 after deleting harmonics in grid voltage and increase the amplitude of grid voltage by 5% to reach 327volt at t=0.2sec …….……..……..41

Figure 42: Grid current error as function of time in case SMC for c_3=40 with decreasing grid voltage amplitude by 10% to reach 280volt……....……42

Figure 43: Grid current error as function of time in case SMC for c_3=40 with decreasing grid voltage amplitude by 10% to reach 280volt with inserting 3rd and 5th harmonics in grid voltage and also increase reference grid current from 35A to 40A.…….....42

Figure 44: Grid current and grid voltage as function of time in case SMC for c_3=40 with different disturbances in grid reference current and grid voltage.…….....43

Figure 45: Grid current and grid current reference as function of time in case SMC for c_3=40 with difference disturbances in grid voltage and grid current reference....43

Figure 46: Grid current error as function of time in case SMC and MRC for c_3=40 and Kr=40 after insertion disturbance by decreasing I2ref from 35A to 25A…..…..44

Figure 47: Grid current error as function of time in case SMC and MRC for c_3=40 and Kr=40 after insertion decreasing I2ref from 35A to 25A. ……...…...44

Figure 48: Grid current error as function of time in case SMC and MRC for c_3=40 and Kr=30.…….……..……..…….…45

Figure 49: Grid current error as function of time in case SMC and MRC for Kr=30 with decreasing the grid reference current from 35A to 25A.…….……..…45

Figure 50: Grid current error as function of time in case of SMC and IC for Ki=10^4..……...……...46

Figure 51: Grid current error as function of time in case of SMC and IC for Ki=10^4 after decreasing I2ref from 35A to 25A……..……46

Figure 52: Grid current error as function of time in case of SMC, IC, and MRC for Ki=10^4 and Kr=30 for different disturbances occurred in grid voltage and grid reference current.……...……...…….47

Figure 53: Grid current error as function of time in case of SMC, IC, and MRC for Ki=10^4 and Kr=30 after decreasing I2ref from 35A to 25A……..…..……...47

Figure 54: Grid current and grid voltage (scaled by 1/7) as function of time in case of SMC, IC, and MRC for Ki=10^4 and Kr=30 for different disturbances occurred in grid voltage and grid reference current…….....……48

Figure 55: Grid current and grid current reference as function of time in case of SMC, IC, and MRC for Ki=$10^4$and Kr=30 for different disturbances occurred in grid voltage and grid reference current……..……48

Figure 56: Total harmonic distortion in grid current as function of time in case of SMC, IC, and MRC for Ki=10^4 and Kr=30 for different disturbances occurred in grid voltage and grid reference current…….....……...49

LIST OF SYMBOLS

L_{1e}	Estimated value of the inductor at inverter side (mH)
L_{2e}	Estimated value of the inductor at grid side (mH)
C_e	Estimated value of the capacitor filter (μF)
r_{1e}	Estimated value of the resistance for inductor at inverter side (Ω)
r_{2e}	Estimated value of the resistance for inductor at inverter side (Ω)
L_{1a}	Actual value of the inductor at inverter side (mH)
L_{2a}	Actual value of the inductor at grid side (mH)
C_a	Actual value of the capacitor filter (μF)
r_{1a}	Actual value of the resistance for inductor at inverter side (Ω)
r_{2a}	Actual value of the resistance for inductor at grid side (Ω)
ΔL_1	Uncertainty term in inductor at inverter side (mH)
ΔL_2	Uncertainty term in inductor at grid side (mH)
ΔC	Uncertainty term in capacitor filter (μF)
Δr_1	Uncertainty term in the resistance of inductor at inverter side (Ω)
Δr_2	Uncertainty term in the resistance of inductor at gird side (Ω)
v_c	Voltage of capacitor filter (Volt)
v_c^*	Reference voltage of capacitor filter (Volt)

i_2	Grid current (Ampere)
i_2^*	Reference for grid current (Ampere)
i_1	Inverter output current (Ampere)
i_1^*	Reference of inverter output current (Ampere)
e_1	Error in the inverter output current (Ampere)
e_2	Error in the capacitor voltage (Volt)
e_3	Error in the grid current (Ampere)
$\mathbf{d}$	Control input of the system
$\mathbf{d_0}$	Initial value of control input of the system
$\mathbf{\Delta d}$	Change in control input of the system after its initial value
V_{dc}	DC voltage (Volt)
v_g	Grid voltage (Volt)
v_{g1}	Fundamental value of grid voltage (Volt)
v_{ng}	Harmonics value of grid voltage (Volt)
w_0	Fundamental frequency (rad/sec)
n	Constant represents the Harmonic terms
K_i	Integral controller gain
K_r	Resonant controller gain
c_1	Positive Constant

c_2	Positive Constant
c_3	Positive Constant
k	Positive Constant
a	Positive Constant
σ	Switching function
$\mathbf{d_L}$	Linear part of control input
$\mathbf{d_{NL}}$	Nonlinear part of control input
$\mathbf{d_{EQ}}$	Equivalent part of control input

LIST OF ABBREVIATIONS

SMC	Sliding mode controller
MRC	Multi-resonant controller
IC	Integral controller
VSI	Voltage source inverter
DC	Direct current
AC	Alternating current
THD	Total harmonic distortion
PWM	Pulse width modulation
PV	Photo voltaic
SSE	Steady state error

Chapter 1

INTRODUCTION

1.1 Inverter

Power converters are the devices which transfer the AC power into the grid where the renewable energy sources like solar PV, wind etc. are interfaced to the existing power supply. This results in the elimination of the transmission and distribution losses and improves reliability of the power supply [1].

Inverter is an electrical device which converts DC into AC. It can be used for different power levels such as powering a car radio to that of backing up a building in case of power outage. DC/AC power converters are mainly used to take DC power supplied by a battery, such as 12V car battery, at its input and transform it into a 220V AC power source operating at 50Hz as an output [3]. A filter is required between inverter and the load. It is used to reduce the harmonics of the output current and plays an important role in the feedback control strategies applied on the inverter to control the sinusoidal current tracking error and total harmonic distortion [4]. Figure 1 describes a circuit diagram for a DC input source and an inverter with LC filter supplying sinusoidal AC power to the load.

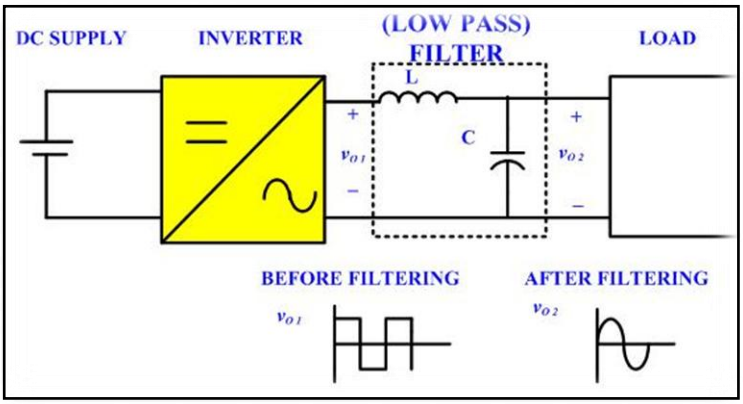

Figure 1: Circuit diagram of an inverter with LC filter connected to the load [5].

Inverters can be categorized according to the types of supply [5]:

1. Voltage Source Inverter (VSI) as shown in Figure 2

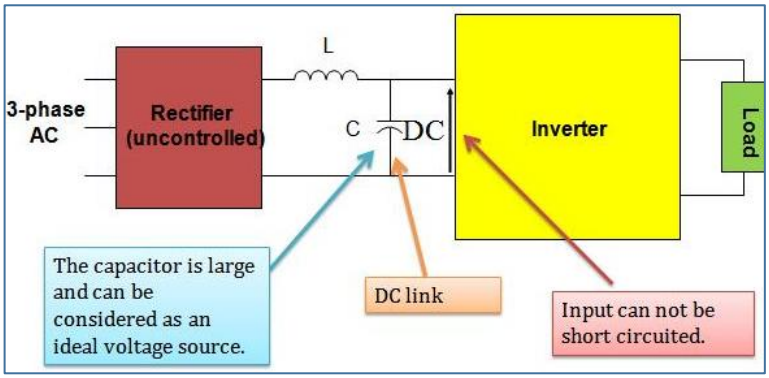

Figure 2: Circuit diagram of voltage source inverter with LC filter with load.

2. Current source inverter (CSI) shown in Figure 3

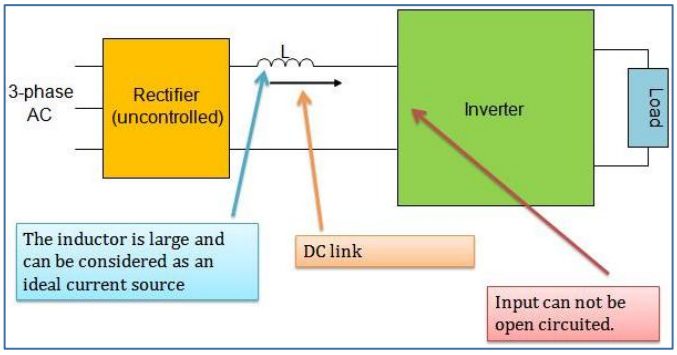

Figure 3: Circuit diagram of current source inverter with L filter connected to the load [5].

3. Voltage source inverter (VSI) with adjustable DC link

This type of inverters can be used with variable input DC link supply using choppers as DC/DC converter as shown in Figure 4. The output is a variable square wave voltage as shown in Figure 5. Also, the frequency of the output voltage can be variable by changing the frequency of the square wave pulses. The waveform are simple but poor total harmonic distortion for this method makes it not reliable [6].

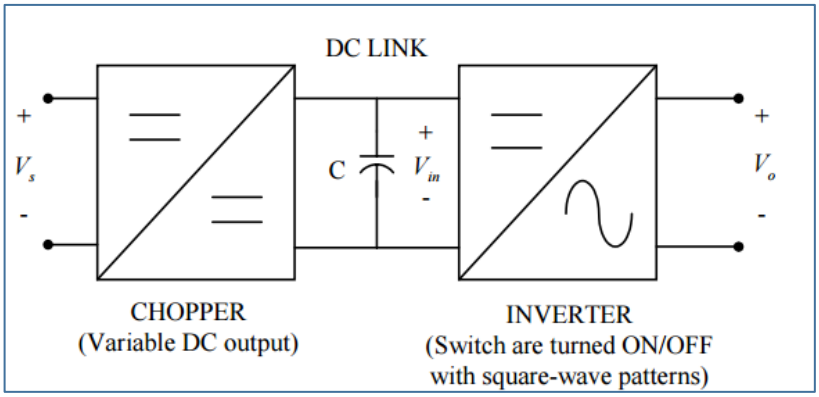

Figure 4: Circuit diagram of voltage source inverter with LC filter connected to the load with variable DC supply at its input terminal [6].

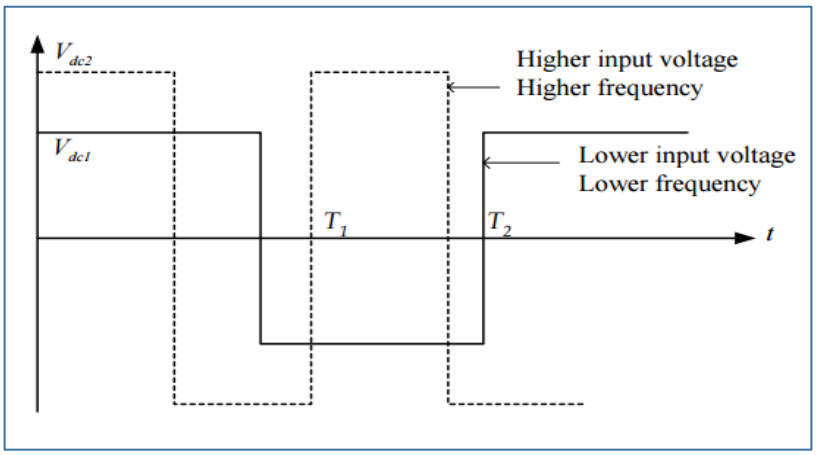

Figure 5: Variable square wave form for the inverter output voltage according to variable input DC supply [6].

4. Voltage source inverter (VSI) with constant DC link

In this type of inverters, the DC link is kept constant .The output voltage and frequency can be varied by using PWM technique as shown in Figure 6. This method has better harmonic distortion but more complex waveform.

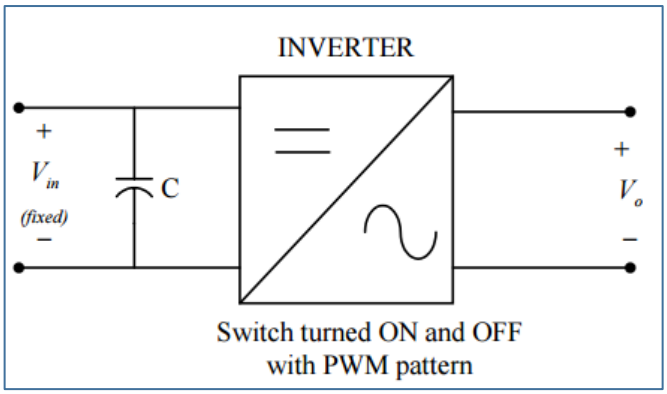

Figure 6: Circuit diagram of voltage source inverter with fixed DC supply at its input terminal [6].

1.1.1 Single Phase Half Bridge Inverter

The capacitors must have the same value. This means that the DC link is equally divided into two. If the top switch S1 is ON, then the bottom switch must be OFF, this results in square wave output voltage as shown in Figure 7.

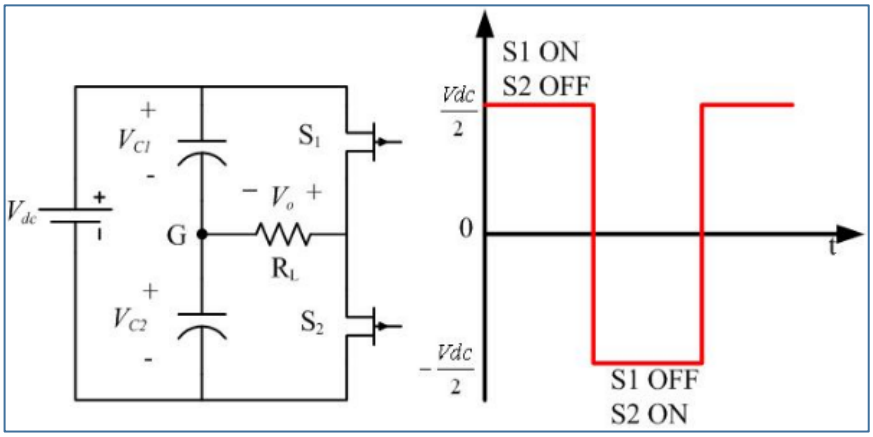

Figure 7: Circuit diagram of single phase half bridge voltage source inverter with fixed DC supply at its input terminal and the waveform of its output voltage [5].

1.1.2 Single Phase Full Bridge Inverter

This inverter consists of two half-bridge legs as shown in Figure 8 where the switching in the second leg is delayed by 180 degrees from the first leg.

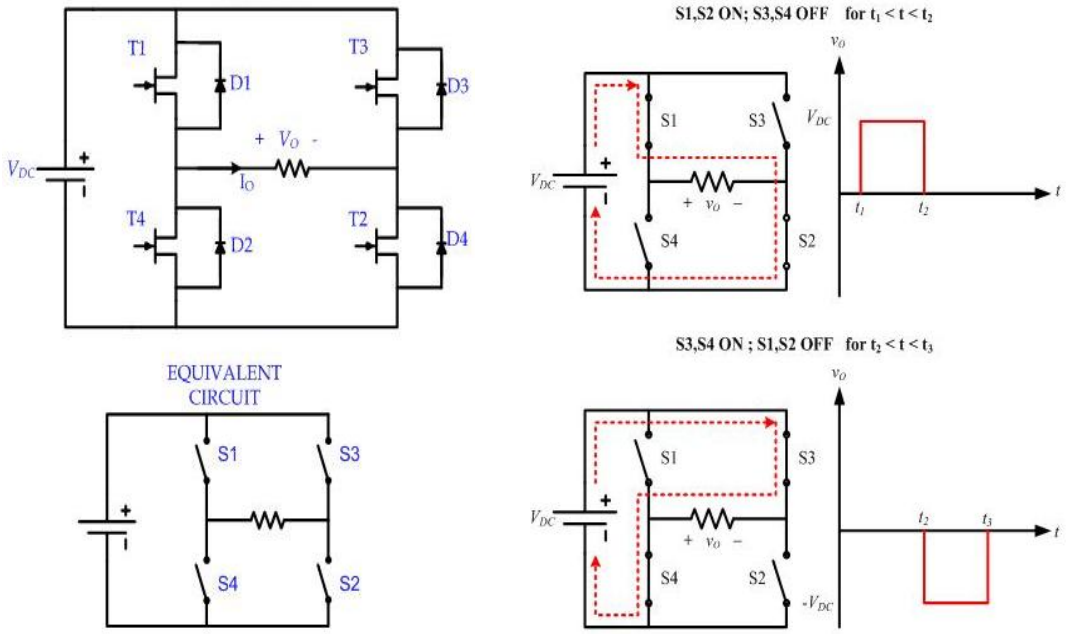

Figure 8: Circuit diagram of single phase full bridge voltage source inverter with fixed DC supply at its input terminal and the waveform of its output voltage [5].

1.1.3 Three Phase Inverter

Three phase inverters are used to supply three phase power to a three phase load either connected in star or delta connection as shown in Figure 9. This types of inverters consists of three similar legs in which one of the switches in each leg must be on and the other is off. So, the output voltage depends on the applied input DC voltage and the status of the switch. We conclude that the output voltage is independent of the load current [7]. Figure 10 shows a three level output voltage on phase A.

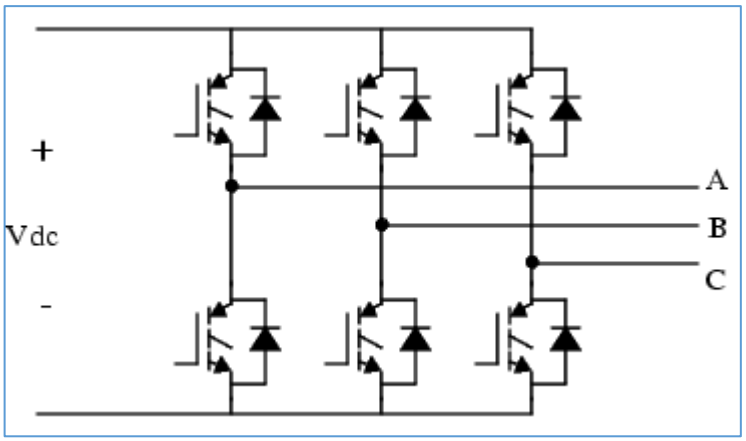

Figure 9: Circuit diagram of three phase voltage source inverter with fixed DC supply at its input terminal [7].

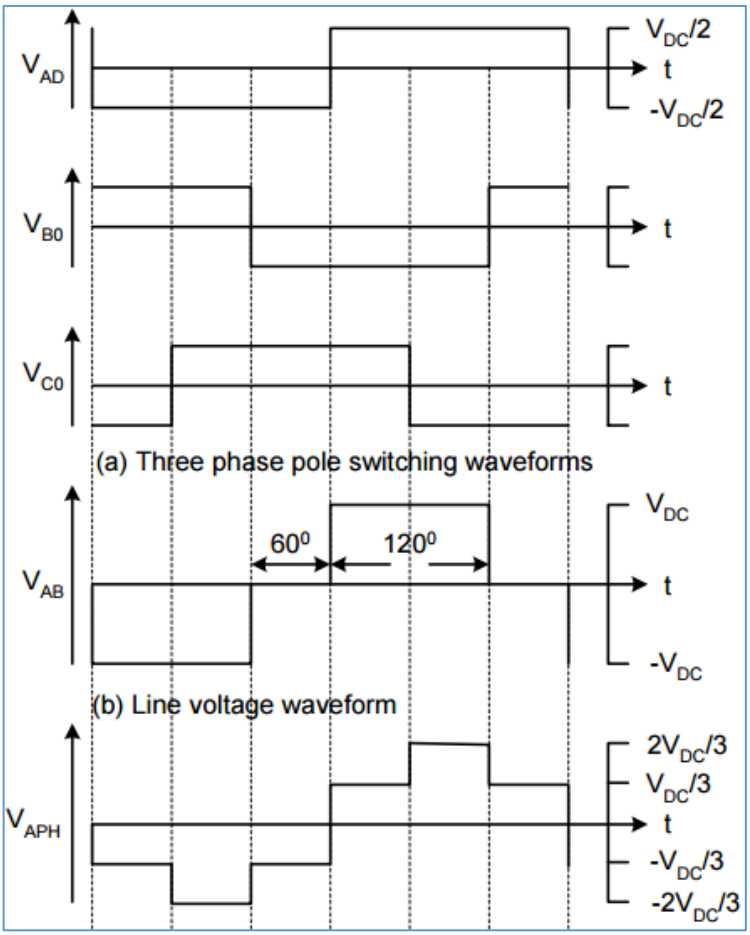

Figure 10: Output voltage waveform of three phase voltage source inverter with fixed DC supply at its input terminal [6].

1.1.4 Pulse Width Modulation (PWM)

For converters to operate, the switches need to be triggered. Pulse width modulation is used to trigger the switches of the converter circuits. Triangulation method (Natural sampling) is used in which the amplitude of the triangular wave (carrier) and sine wave (modulating) are compared to obtain the PWM waveform as shown in Figure 11. In the industries, they widely used the digital method to obtain PWM and it is called regular sampling [8].

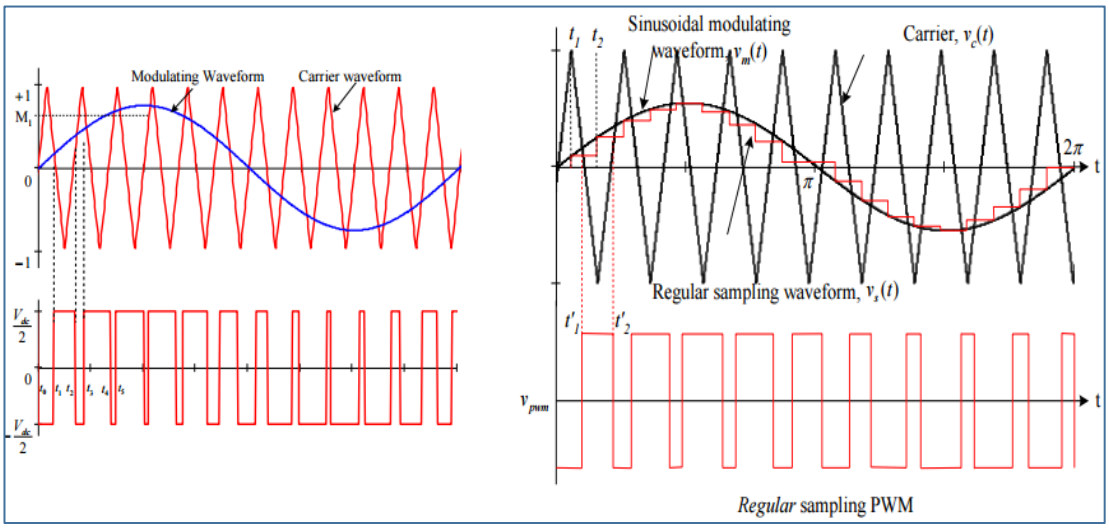

Figure 11: Method of operation of PWM technique [10].

1.2 Thesis Contribution

For the voltage source grid connected inverters to act with a high performance, an inductor-capacitor-inductor (LCL) filter is used to perform attenuation for the switching noise at a smaller size of filter components as compared with an inductor (L-type) filter (an LCL-type filter is a more compact option with lower cost and losses) [2].

Inverter, LCL filter, and a special feedback controller should achieve a pure sinusoidal grid current with a very low total harmonic distortion, a fast transient response for sudden load and high efficiency.

The topic of this thesis is to discuss a control method which improves the above factors such that the inverter's efficiency is increased. Chapter1 gives an introduction about inverter and its application while chapter 2 gives an overview of a system represented by input DC source and grid connected voltage source inverter with LCL filter. In this chapter, we will define the parameters and the terms presented in the system. Chapter 3 discusses the applied control strategy the sliding mode controller (SMC) in this system and the determination of the control input in this system. Chapter 4 shows the performance of the system theoretically in case of sliding mode controller (SMC) alone and after the addition of the integral controller (IC) and when we add sliding mode controller (SMC), integral controller (IC) and mutli-resonant terms controller (MRC) together. Chapter 5 shows the proposed model implemented using mat-lab Simulink 2015 and the results of the simulations in four case are SMC lone, (SMC and IC), (SMC and MRC), and (SMC, IC, and MRC). These result are compared to the work of another paper from IEEE transaction in [11]. Chapter 6 ends this thesis with a conclusion and the future work.

Chapter 2

GRID CONNECTED INVERTER WITH LCL FILTER

2.1 System Definition

The circuit below describes a system which consists of an input DC source and grid connected voltage source inverter (VSI) with LCL filter as shown in figure 12. The LCL filter consists of a capacitor that divides the inductor into L1 and L2 at the inverter side and grid side. Each inductor has a small resistance (assumed to be 0.01Ω) while the resistane of the capacitor is neglected.

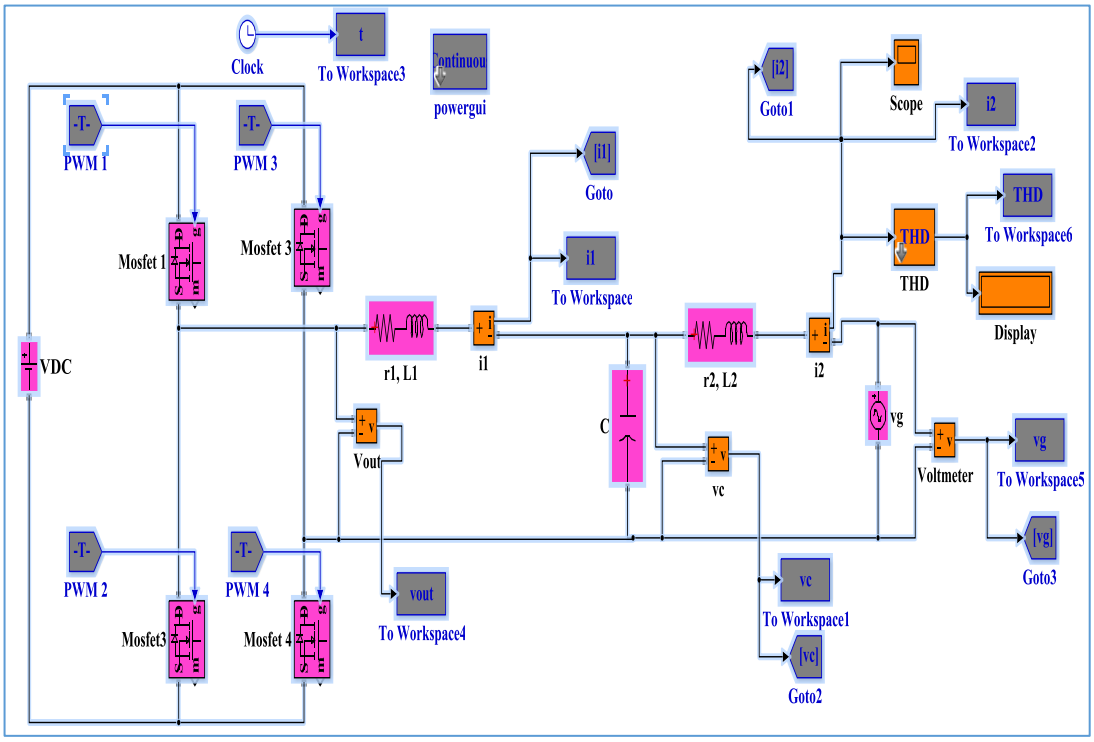

Figure 23: Single phase grid connected VSI with LCL filter

2.1.1 Reference Functions

In every system, the desired results are considered as references. From Figure 12, equation (1) can be determined by taking the voltage loop in circuit 1 which contains the inverter output voltage, the capacitor, and the inductor L1 at the inverter side.Also, equation (2) can be determined by applying a voltage loop in circuit 2 which contains the capacitor, the inductor L2 at the grid side, and the grid voltage. Equation (3) can be determined by applying KCL rule at the node separating the filter parameters.

$$L_{1a}\frac{di_1}{dt} + r_{1a}i_1 = \mathbf{d}V_{dc} - v_c \tag{1}$$

$$L_{2a}\frac{di_2}{dt} + r_{2a}i_2 = v_c - v_g \tag{2}$$

$$C_a\frac{dv_c}{dt} = i_1 - i_2 \tag{3}$$

where i_1 and i_2 are the inverter output current and the grid current.

v_c and v_g are the capacitor voltage and the grid voltage.

L_{1a}, L_{2a}, and C_a are the actual values of the filter inductors.

r_{1a} and r_{2a} are the actual resistance values for the filter inductors.

d is the control input of the system.

Then from (1), (2), and (3) we have the following reference functions:

$$i_2^* = I_2\sin\left(w_0 t\right) \tag{4}$$

$$v_c^* = L_{2e}\frac{di_2^*}{dt} + r_{2e}i_2^* + v_g \tag{5}$$

$$i_1^* = i_c^* + i_2^* = C_e \frac{dv_c^*}{dt} + i_2^* \tag{6}$$

$$\Rightarrow i_1^* = L_{2e} C_e \frac{di_2^{*2}}{dt^2} + C_e r_{2e} \frac{di_2^*}{dt} + C_e \frac{dv_g}{dt} + i_2^* \tag{7}$$

where i_2^* is the grid current reference.

v_c^* is the voltage capacitor reference.

i_1^* is the output current inverter reference.

L_{1e}, L_{2e}, and C_e are the estimated values of the filter inductors.

r_{1e} and r_{2e} are the estimated resistance values for the filter inductors.

2.1.2 Steady State Errors

The errors in the system can be represented by

$$e_1 = i_1 - i_1^* \tag{8}$$

$$e_2 = v_c - v_c^* \tag{9}$$

$$e_3 = i_2 - i_2^* \tag{10}$$

where e_1 is the error in the inverter output current.

e_2 is the error in the capacitor voltage.

e_3 is the tracking error in the sinusoidal grid current.

2.1.3 Uncertainty Parameters

The values of the parameters of the filter (L1, L2, and C) have uncertainty values assumed to be 25% from their estimated values. These uncertainty parameters can be represented by

$$\Delta L_1 = L_{1e} - L_{1a} \tag{11}$$

$$\Delta L_2 = L_{2e} - L_{2a} \tag{12}$$

$$\Delta C = C_e - C_a \tag{13}$$

$$\Delta r_1 = r_{1e} - r_{1a} \tag{14}$$

$$\Delta r_2 = r_{2e} - r_{2a} \tag{15}$$

where ΔL_1, ΔL_2, ΔC, Δr_1, and Δr_2 are the uncertainty values between estimated and the actual values of the filter parameters.

2.1.4 Control Input

Let the control input of the system to be

$$\mathbf{d} = \mathbf{d_0} + \mathbf{\Delta d} \tag{16}$$

$$\mathbf{d_0} = \left[L_{1e} \frac{di_1^*}{dt} + r_{1e} i_1^* + v_c^* \right] \frac{1}{V_{dc}} \tag{17}$$

where d is the control input of the system, $\mathbf{d_0}$ is the control input of the system at the steady state mode, and $\mathbf{\Delta d}$ is the control input of the system before reaching steady state mode.

2.2 Representing The System In State - Space Model

To represent a given system in state - space model, we should describe the states in this system.

The states in our system are

$$\dot{\mathbf{E}} = \begin{bmatrix} \dot{e}_1(t) \\ \dot{e}_2(t) \\ \dot{e}_3(t) \end{bmatrix} \tag{18}$$

where the above states describes the error change as function of time in the inverter output current, the capacitor voltage, and the grid current. We will derive the states of the system including the parameters of the system as shown below:

$$from(1)$$

$$L_{1a}\frac{di_1}{dt}+r_{1a}i_1=(\mathbf{d_0}+\mathbf{\Delta d})V_{dc}-v_c$$

$$L_{1a}\frac{di_1}{dt}+r_{1a}i_1=L_{1e}\frac{di_1^*}{dt}+r_{1e}i_1^*+v_c^*+\mathbf{\Delta d}V_{dc}-v_c$$

$$L_{1a}\frac{di_1}{dt}+r_{1a}i_1-r_{1e}i_1^*=L_{1e}\frac{di_1^*}{dt}-e_2(t)+\mathbf{\Delta d}V_{dc}$$

$$L_{1a}\frac{di_1}{dt}-L_{1e}\frac{di_1^*}{dt}+r_{1a}i_1-r_{1e}i_1^*=-e_2(t)+\mathbf{\Delta d}V_{dc}$$

$$L_{1a}\frac{di_1}{dt}-L_{1a}\frac{di_1^*}{dt}+L_{1a}\frac{di_1^*}{dt}-L_{1e}\frac{di_1^*}{dt}+r_{1a}i_1-r_{1a}i_1^*+r_{1a}i_1^*-r_{1e}i_1^*$$
$$=-e_2(t)+\mathbf{\Delta d}V_{dc}$$

$$L_{1a}\frac{di_1}{dt}-\Delta L_1\frac{di_1^*}{dt}-L_{1a}\frac{di_1^*}{dt}+r_{1a}i_1-\Delta r_1 i_1^*-r_{1a}i_1^*$$
$$=-e_2(t)+\mathbf{\Delta d}V_{dc}$$

$$L_{1a}\dot{e_1}(t)-\Delta L_1\frac{di_1^*}{dt}+r_{1a}e_1(t)-\Delta r_1 i_1^*=-e_2(t)+\mathbf{\Delta d}V_{dc}$$

$$L_{1a}\dot{e_1}(t)=\Delta L_1\frac{di_1^*}{dt}-r_{1a}e_1(t)+\Delta r_1 i_1^*-e_2(t)+\mathbf{\Delta d}V_{dc} \quad (19)$$

Equation (19) describes the change of the error in the output inverter current as function of the time depending on the parameters of the system

$$from(2)$$

$$L_{2a}\frac{di_2}{dt}+r_{2a}i_2=v_c-v_g$$

$$L_{2a}\frac{di_2}{dt}+r_{2a}i_2=e_2(t)+v_c^*-v_g$$

$$L_{2a}\frac{di_2}{dt}+r_{2a}i_2=e_2(t)+L_{2e}\frac{di_2^*}{dt}+r_{2e}i_2^*+v_g-v_g$$

$$L_{2a}\frac{di_2}{dt}-L_{2a}\frac{di_2^*}{dt}+L_{2a}\frac{di_2^*}{dt}+r_{2a}i_2-r_{2a}i_2^*+r_{2a}i_2^*=e_2(t)+L_{2e}\frac{di_2^*}{dt}+r_{2e}i_2^*$$

$$L_{2a}\dot{e_3}(t)+(L_{2a}-L_{2e})\frac{di_2^*}{dt}+r_{2a}e_3(t)+i_2^*(r_{2a}-r_{2e})=e_2(t)$$

$$L_{2a}\dot{e_3}(t)=\Delta L_2\frac{di_2^*}{dt}-r_{2a}e_3(t)+\Delta r_2 i_2^*+e_2(t) \quad (20)$$

Equation (19) describes the change of the error in the grid current as function of time depending on the parameters of the system

$$from(3)$$

$$C_a \frac{dv_c}{dt} = i_1 - i_2$$

$$C_a \frac{dv_c}{dt} = i_1 - i_1^* + i_1^* - \left(i_2 - i_2^* + i_2^*\right)$$

$$C_a \frac{dv_c}{dt} = e_1(t) - e_3(t) + i_1^* - i_2^*$$

$$C_a \frac{dv_c}{dt} - C_a \frac{dv_c^*}{dt} + C_a \frac{dv_c^*}{dt} = e_1(t) - e_3(t) + i_1^* - i_2^*$$

$$C_a \dot{e}_2(t) = e_1(t) - e_3(t) + i_1^* - i_2^* - C_a \frac{dv_c^*}{dt}$$

$$C_a \dot{e}_2(t) = e_1(t) - e_3(t) + L_{2e} C_e \frac{di_2^{*2}}{dt^2} + C_e r_{2e} \frac{di_2^*}{dt} + C_e \frac{dv_g}{dt} - C_a L_{2e} \frac{di_2^{*2}}{dt^2} - C_a r_{2e} \frac{di_2^*}{dt} - C_a \frac{dv_g}{dt}$$

$$C_a \dot{e}_2(t) = e_1(t) - e_3(t) + (C_e - C_a) L_{2e} \frac{di_2^{*2}}{dt^2} + (C_e - C_a) r_{2e} \frac{di_2^*}{dt} + (C_e - C_a) \frac{dv_g}{dt}$$

$$C_a \dot{e}_2(t) = e_1(t) - e_3(t) + \Delta C L_{2e} \frac{di_2^{*2}}{dt^2} + \Delta C r_{2e} \frac{di_2^*}{dt} + \Delta C \frac{dv_g}{dt}$$

$$C_a \dot{e}_2(t) = e_1(t) - e_3(t) + \Delta C \left(L_{2e} \frac{di_2^{*2}}{dt^2} + r_{2e} \frac{di_2^*}{dt} + \frac{dv_g}{dt} \right)$$

$$C_a \dot{e}_2(t) = e_1(t) - e_3(t) + \Delta C \frac{dv_c^*}{dt} \tag{21}$$

Equation (20) describes the change of the error in the capacitor voltage as function of the parameters of the system.

After organizing equations (19), (20), and (21) in a matrix form we have

$$\dot{\mathbf{E}} = \begin{bmatrix} \dot{e}_1(t) \\ \dot{e}_2(t) \\ \dot{e}_3(t) \end{bmatrix} = \mathbf{AE} + \mathbf{B\Delta d} + \mathbf{D} \tag{22}$$

where matrices **A**, **E**, **B**, and **D** are defined as follows:

$$\dot{\mathbf{E}} = \begin{bmatrix} \frac{-r_{1a}}{L_{1a}} & \frac{-1}{L_{1a}} & 0 \\ \frac{1}{C_a} & 0 & \frac{-1}{C_a} \\ 0 & \frac{1}{L_{2a}} & \frac{-r_{2a}}{L_{2a}} \end{bmatrix} \begin{bmatrix} e_1(t) \\ e_2(t) \\ e_3(t) \end{bmatrix} + \begin{bmatrix} \frac{V_{dc}}{L_{1a}} & 0 & 0 \\ 0 & 0 & 0 \\ 0 & 0 & 0 \end{bmatrix} \begin{bmatrix} \mathbf{\Delta d} \\ 0 \\ 0 \end{bmatrix} + \begin{bmatrix} \frac{\Delta r_1 i_1^*}{L_{1a}} + \frac{\Delta L_1 \frac{di_1^*}{dt}}{L_{1a}} \\ \frac{\Delta C}{C_a} \frac{dv_c^*}{dt} \\ \frac{\Delta L_2}{L_{2a}} \frac{di_2^*}{dt} + \frac{\Delta r_2}{L_{2a}} i_2^* \end{bmatrix} \tag{23}$$

Equation (23) represents our system in the state-space model

Chapter 3

SLIDING MODE CONTROL STRATEGY

3.1 Theory Of Operation Of Sliding Mode Controller

Sliding mode control (SMC) is a nonlinear control technique which is characterized by the accuracy, robustness, tuning and easy implementation. SMC technique forces the states of the system to reach and remain on a surface which called sliding surface until reaching equilibrium point or steady state [9].

SMC design involves two steps:

1. Selection of a special or stable sliding surface in which switching is occurred. This sliding surface can be represented by the switching function σ which is a linear combination of the states of the system [10].

$$\sigma = \mathbf{CE} = \begin{bmatrix} c_1 & c_2 & c_3 \end{bmatrix} \begin{bmatrix} e_1(t) \\ e_2(t) \\ e_3(t) \end{bmatrix} = c_1 e_1(t) + c_2 e_2(t) + c_3 e_3(t) \tag{24}$$

where c_1, c_2, and c_3 are positive numbers

2. Control law which makes the selected sliding surface or switching surface attractive and achieve the stability [10]. But SMC suffers from chattering phenomena corresponds to the vibrations around the sliding surface that causes current harmonics, electromagnetic interference, and increases the power losses in the system. In order to suppress the chattering in SMC, Gao et al in [11] presented a reaching mode in form of equation

$$\dot{\sigma} = \mathbf{C}\dot{\mathbf{E}} = \mathbf{CAE} + \mathbf{CB}\Delta\mathbf{d} + \mathbf{CD} = -k\sigma - \varepsilon \operatorname{sgn}(\sigma) \tag{25}$$

Where k is a positive number for achieving the stability in the system, ε is also a positive number for accelerating the reaching mode, and $\operatorname{sgn}(\sigma)$ is the sign function for the switching function σ.

Figure 13 can summarizes step 1 and step 2. The black lines are the states of the system $e_1(t)$ and $e_3(t)$ considering that $e_2(t)$ value is negligible. The red line corresponds to the selected sliding surface or switching function σ as mentioned in step 1. The two blue curved lines with arrow corresponds to the reachability mode that is mentioned in step 2.

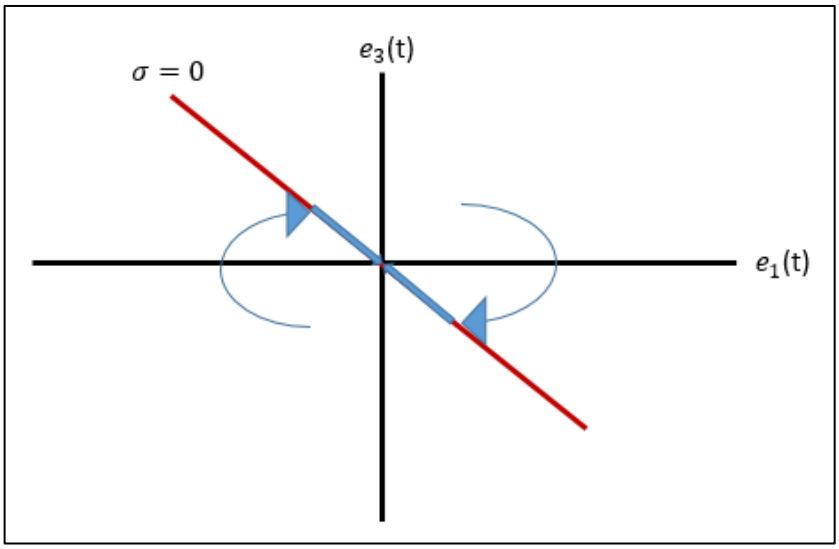

Figure 13: Theory of operation of sliding mode control

3.1.1 Control Input Determination

Substitute (23) and (24) in (25) we have:

$$
\begin{aligned}
&\frac{1}{L_{1a}}\left(c_1\Delta L_1\frac{di_1^*}{dt}-c_1r_{1a}e_1(t)+c_1\Delta r_1i_1^*-c_1e_2(t)+c_1\mathbf{\Delta d}V_{dc}\right)\\
&+\frac{1}{L_{2a}}\left(c_3\Delta L_2\frac{di_2^*}{dt}-c_3r_{2a}e_3(t)+c_3\Delta r_2i_2^*+c_3e_2(t)\right)\\
&+\frac{1}{C_a}\left(c_2e_1(t)-c_2e_3(t)+c_2\Delta C\frac{dv_c^*}{dt}\right)=-k\sigma-\varepsilon\,\mathrm{sgn}(\sigma)\\
&e_1(t)\left(\frac{c_2}{C_a}-\frac{c_1r_{1a}}{L_{1a}}\right)+e_2(t)\left(\frac{-c_1}{L_{1a}}+\frac{c_3}{L_{2a}}\right)+e_3(t)\left(\frac{-c_2}{C_a}-\frac{c_3r_{2a}}{L_{2a}}\right)+i_1^*\left(\frac{c_1\Delta r_1}{L_{1a}}\right)\\
&+\frac{di_1^*}{dt}\left(\frac{c_1\Delta L_1}{L_{1a}}\right)+i_2^*\left(\frac{c_3\Delta r_2}{L_{2a}}\right)+\frac{di_2^*}{dt}\left(\frac{c_3\Delta L_2}{L_{2a}}\right)+\frac{dv_c^*}{dt}\left(\frac{c_2\Delta C}{C_a}\right)\\
&+k\sigma+\varepsilon\,\mathrm{sgn}(\sigma)=\frac{-c_1\mathbf{\Delta d}V_{dc}}{L_{1a}}
\end{aligned}
\tag{26}
$$

After organizing equation (24), the control input of the system $\mathbf{\Delta d}$ before reaching steady state can be determined

$$
\begin{aligned}
\Delta dV_{dc}&=e_1\left(\frac{-L_{1a}c_2}{c_1C_a}+r_{1a}\right)+e_2\left(1-\frac{L_{1a}c_3}{c_1L_{2a}}\right)+e_3\left(\frac{L_{1a}c_2}{c_1C_a}+\frac{L_{1a}c_3r_{2a}}{c_1L_{2a}}\right)\\
&-i_1^*\Delta r_1-\dot{i}_1^*\,\Delta L_1+i_2^*\left(-\frac{L_{1a}c_3\Delta r_2}{c_1L_{2a}}\right)+\dot{i}_2^*\left(-\frac{L_{1a}c_3\Delta L_2}{c_1L_{2a}}\right)\\
&+\dot{V}_c^*\left(-\frac{L_{1a}c_2\Delta C}{c_1C}\right)-\frac{L_{1a}}{c_1}k\sigma-\frac{L_{1a}}{c_1}\varepsilon\,\mathrm{sgn}(\sigma)
\end{aligned}
\tag{27}
$$

SMC path starting from a non-zero initial condition develops in two phases which are:

a) Reaching mode, in which it reaches the sliding surface.

b) Sliding mode, in which the states of the system and the path of reaching sliding surface stays on the sliding surface and develops according to the dynamic situations of the system.

Therefore, the control input which is responsible for the trajectories of SMC can be divided into two parts:

- $\mathbf{d_L}$ and $\mathbf{d_{NL}}$ are called the linear and non-linear corrective parts of the control input shown in equation (28) and (29) : correct the deviations from the sliding surface
- $\mathbf{d_{EQ}}$ is equivalent part of the control input shown in equation (30) : makes the derivative of the sliding surface zero to stay on the sliding surface.

Equation (27) can be divided into three parts

$$\mathbf{d_L} V_{dc} = -\frac{L_{1a}}{c_1} k\sigma \tag{28}$$

$$\mathbf{d_{NL}} V_{dc} = -\frac{L_{1a}}{c_1} \varepsilon \operatorname{sgn}(\sigma) \tag{29}$$

$$\begin{aligned}\mathbf{d_{EQ}} V_{dc} = {} & e_1(t)\left(\frac{-L_{1a}c_2}{c_1 C_a} + r_{1a}\right) + e_2(t)\left(1 - \frac{L_{1a}c_3}{c_1 L_{2a}}\right) + e_3(t)\left(\frac{L_{1a}c_2}{c_1 C_a} + \frac{L_{1a}c_3 r_{2a}}{c_1 L_{2a}}\right) \\ & -i_1^{*}\Delta r_1 - \frac{di_1^{*}}{dt}\Delta L_1 + i_2^{*}\left(-\frac{L_{1a}c_3\Delta r_2}{c_1 L_{2a}}\right) + \frac{di_2^{*}}{dt}\left(-\frac{L_{1a}c_3\Delta L_2}{c_1 L_{2a}}\right) + \frac{dv_c^{*}}{dt}\left(-\frac{L_1 c_2 \Delta C}{c_1 C_a}\right)\end{aligned} \tag{30}$$

We should note that during the implementation of the control input **d** experimentally, the uncertainty values shouldn't be considered because they are variable and their values are unknown. But in this thesis, we take the uncertainty values to be 25% as an example so we can notice the grid current error during simulation.

We can see from (28) and (29) that the linear and non-linear parts of control input (d_L and d_{NL}) depend on the switching function σ since they are responsible for reaching mode. Also, from (30) we can see that the equivalent part of control input is independent of the switching function σ since it is responsible for the sliding mode on sliding surface until reaching equilibrium point at zero.

The total control input of the system can be determined by adding equations (17), (28), (29), and (30) to get equation (31)

$$\mathbf{d}V_{dc} = \mathbf{d_0}V_{dc} + \Delta\mathbf{d}V_{dc} = \left[L_{1e}\frac{di_1^*}{dt} + r_{1e}i_1^* + v_c^* \right] + e_1(t)\left(\frac{-L_{1a}c_2}{c_1C_a} + r_{1a} \right)$$
$$+e_2(t)\left(1 - \frac{L_{1a}c_3}{c_1L_{2a}} \right) + e_3(t)\left(\frac{L_{1a}c_2}{c_1C} + \frac{L_{1a}c_3r_{2a}}{c_1L_{2a}} \right) - i_1^*\Delta r_1 - \frac{di_1^*}{dt}\Delta L_1$$
$$+i_2^*\left(-\frac{L_{1a}c_3\Delta r_2}{c_1L_{2a}} \right) + \frac{di_2^*}{dt}\left(-\frac{L_{1a}c_3\Delta L_2}{c_1L_{2a}} \right) + \frac{dv_c^*}{dt}\left(-\frac{L_{1a}c_2\Delta C}{c_1C_a} \right) \quad (31)$$
$$-\frac{L_{1a}}{c_1}k\sigma - \frac{L_{1a}}{c_1}\varepsilon\,\mathrm{sgn}(\sigma)$$

Defining the constants in equation (31), we get control input of the system in (38)

$$K_1 = \frac{-L_{1a}c_2}{c_1C_a} + r_{1a} \quad (32)$$

$$K_2 = 1 - \frac{L_{1a}c_3}{c_1L_{2a}} \quad (33)$$

$$K_3 = \frac{L_{1a}c_2}{c_1C_a} + \frac{L_{1a}c_3r_{2a}}{c_1L_{2a}} \quad (34)$$

$$K_4 = -\frac{L_{1a}c_3\Delta r_2}{c_1L_{2a}} \quad (35)$$

$$K_5 = -\frac{L_{1a}c_3\Delta L_2}{c_1L_{2a}} \quad (36)$$

$$K_6 = -\frac{L_{1a}c_2\Delta C}{c_1C_a} \quad (37)$$

$$\mathbf{d}V_{dc} = \mathbf{d_0}V_{dc} + \Delta\mathbf{d}V_{dc} = \left[L_{1e}\frac{di_1^*}{dt} + r_{1e}i_1^* + v_c^* \right] + e_1(t)(K_1)$$
$$+e_2(t)(K_2) + e_3(t)(K_3) - i_1^*\Delta r_1 - \frac{di_1^*}{dt}\Delta L_1$$
$$+i_2^*(K_4) + \frac{di_2^*}{dt}(K_5) + \frac{dv_c^*}{dt}(K_6)$$
$$-\frac{L_{1a}}{c_1}k\sigma - \frac{L_{1a}}{c_1}\varepsilon\,\mathrm{sgn}(\sigma)$$
(38)

Chapter 4

THE CONTROLLERS OF THE SYSTEM

4.1 The Operated Controllers In The System

In this system, the three different controllers are the sliding mode controller (SMC), Integral controller (IC), and Multi-resonant controller (MRC). In this chapter, simulating the steady state response of the grid current error for three different controllers in four cases have been done. The first case done using SMC lone while SMC with MRC is the second case. The third case accomplished by using SMC with integral controller (IC) whereas the fourth case is the addition of all controllers together (SMC, IC, and MRC). During simulation disturbances are injected to prove the ability of the system to reject all the applied external disturbances in the system. The theoretical results in each case are shown in this chapter.

4.1.1 Sliding Mode Controller (SMC)

At steady state:

$$\sigma = c_1 e_1(t) + c_2 e_2(t) + c_3 e_3(t) = 0 \tag{39}$$

We should find the expressions for $e_1(t)$ and $e_2(t)$ in terms of $e_3(t)$. Then from (2) and (3) we can express the error in the output inverter current $e_1(t)$ as function of grid current reference, grid current error, and the grid voltage.

$$e_1(t) = i_1 - i_1^* = C_a \frac{dv_c}{dt} + i_2 - L_{2e}C_e \frac{di_2^{*2}}{dt^2} - r_{2e}C_e \frac{di_2^*}{dt} - C_e \frac{dv_g}{dt} - i_2^*$$

$$e_1(t) = C_a L_{2a} \frac{di_2^{\ 2}}{dt^2} + C_a r_{2a} \frac{di_2}{dt} + C_a \frac{dv_g}{dt} + e_3(t) - L_{2e}C_e \frac{di_2^{*2}}{dt^2} - r_{2e}C_e \frac{di_2^*}{dt} - C_e \frac{dv_g}{dt}$$

$$e_1(t) = C_a L_{2a} \frac{di_2^{\ 2}}{dt^2} + C_a L_{2a} \frac{di_2^{*2}}{dt^2} - C_a L_{2a} \frac{di_2^{*2}}{dt^2} + C_a r_{2a} \frac{di_2}{dt} + C_a r_{2a} \frac{di_2^*}{dt} + C_a r_{2a} \frac{di_2^*}{dt}$$

$$-\Delta C \frac{dv_g}{dt} + e_3(t) - L_{2e}C_e \frac{di_2^{*2}}{dt^2} - r_{2e}C_e \frac{di_2^*}{dt}$$

$$e_1(t) = C_a L_{2a} \ddot{e}_3 + e_3 - \Delta C \dot{v}_g + C_a r_{2a} \dot{e}_3 + \ddot{i}_2^* (L_{2a}C_a - L_{2e}C_e) + \dot{i}_2^* (C_a r_{2a} - r_{2e}C_e) \qquad (40)$$

In the S-domain the error in the output current of the inverter can be expressed as:

$$E_1(s) = C_a L_{2a} s^2 E_3(s) + E_3(s) - \Delta C s V_g(s) + C_a r_{2a} s E_3(s)$$

$$+ s^2 I_2^*(s)(L_{2a}C_a - L_{2e}C_e) + s I_2^*(s)(C_a r_{2a} - r_{2e}C_e)$$

$$E_1(s) = C_a L_{2a} s^2 E_3(s) + E_3(s) - \Delta C s V_g(s) + C_a r_{2a} s E_3(s)$$

$$+ s^2 I_2^*(s) K_7 + s I_2^*(s) K_8$$

$$E_1(s) = E_3(s)\left[C_a L_{2a} s^2 + C_a r_{2a} s + 1\right] + I_2^*(s)\left[K_7 s^2 + K_8 s\right] - \Delta C s V_g(s) \qquad (41)$$

where

$$K_7 = L_{2a}C_a - L_{2e}C_e \qquad (42)$$

$$K_8 = C_a r_{2a} - r_{2e}C_e \qquad (43)$$

Also, from (2) and (3) we can express the error in the capacitor voltage $e_2(t)$ as function of grid current reference and the grid current error.

$$e_2(t) = v_c - v_c^*$$

$$e_2(t) = L_{2a}\frac{di_2}{dt} + r_{2a}i_2 + v_g - L_{2e}\frac{di_2^*}{dt} - r_{2e}i_2^* - v_g$$

$$e_2(t) = L_{2a}\frac{di_2}{dt} - L_{2a}\frac{di_2^*}{dt} + L_{2a}\frac{di_2^*}{dt} + r_{2a}i_2 - r_{2a}i_2^*$$

$$+r_{2a}i_2^* - L_{2e}\frac{di_2^*}{dt} - r_{2e}i_2^*$$

$$e_2(t) = L_{2a}\dot{e}_3 + r_{2a}e_3 + \frac{di_2^*}{dt}(L_{2a} - L_{2e}) + i_2^*(r_{2a} - r_{2e})$$

$$e_2(t) = L_{2a}\dot{e}_3 + r_{2a}e_3 - \frac{di_2^*}{dt}\Delta L_2 - i_2^*\Delta r_2 \tag{44}$$

In the S-domain:-

$$E_2(s) = E_3(s)\left[sL_{2a} + r_{2a}\right] + I_2^*(s)\left[-\Delta L_2 s - \Delta r_2\right] \tag{45}$$

In the S-domain, equation (39) can be rewritten as follows

$$\sigma(s) = c_1E_1(s) + c_2E_2(s) + c_3E_3(s) = 0 \tag{46}$$

Substitute (41) and (45) in equation (46) we have

$$E_3(s)\left[s^2(c_1C_aL_{2a}) + s(c_1C_ar_{2a} + c_2L_{2a}) + (c_1 + c_2r_{2a} + c_3)\right]$$
$$= I_2^*(s)\left[s^2(-c_1K_7) + s(-c_1K_8 + c_2\Delta L_2) + (c_2\Delta r_2)\right] + c_1\Delta CsV_g(s)$$
$$E_3(s)\left[s^2(K_9) + s(K_{10}) + (K_{11})\right]$$
$$= I_2^*(s)\left[s^2(K_{12}) + s(K_{13}) + (K_{14})\right] + K_{15}sV_g(s)$$

$$E_3(s) = \left[\frac{I_2^*(s)\left[s^2(K_{12}) + s(K_{13}) + (K_{14})\right] + K_{15}sV_g(s)}{\left[s^2(K_9) + s(K_{10}) + (K_{11})\right]}\right] \tag{47}$$

Equation (47) describes the grid current error in the s-domain in case of SMC alone where

$$K_9 = c_1C_aL_{2a} \tag{48}$$

$$K_{10} = c_1C_ar_{2a} + c_2L_{2a} \tag{49}$$

$$K_{11} = c_1 + c_2 r_{2a} + c_3 \tag{50}$$

$$K_{12} = -c_1 K_7 \tag{51}$$

$$K_{13} = -c_1 K_8 + c_2 \Delta L_2 \tag{52}$$

$$K_{14} = c_2 \Delta r_2 \tag{53}$$

$$K_{15} = c_1 \Delta C \tag{54}$$

We can define the reference grid current and grid voltage in exponential form:-

$$i_2^* = I_2 \sin\left(w_0 t\right) \tag{55}$$

$$i_2^* = I_2 \left[\frac{e^{jw_0 t} - e^{-jw_0 t}}{2j} \right] \tag{56}$$

$$v_g = v_{1g} \sin\left(w_0 t\right) + v_{ng} \sin\left(n w_0 t\right) \tag{57}$$

$$\dot{v}_g = v_{1g} w_0 \cos\left(w_0 t\right) + v_{ng} n w_0 \cos\left(n w_0 t\right) \tag{58}$$

$$\dot{v}_g = v_{1g} w_0 \left[\frac{e^{jw_0 t} + e^{-jw_0 t}}{2} \right] + v_{ng} n w_0 \left[\frac{e^{jnw_0 t} + e^{-jnw_0 t}}{2} \right] \tag{59}$$

4.1.2 Addition Of Integral Controller

At steady state

$$\sigma = c_1 e_1 + c_2 e_2 + c_3 e_3 + K_i \left(\frac{1}{s} \right) e_3 = 0 \tag{60}$$

where K_i is the integral controller gain

In the S-domain, equation (60) can be rewritten as follows

$$\sigma(s) = c_1 E_1(s) + c_2 E_2(s) + c_3 E_3(s) + K_i \left(\frac{1}{s} \right) E_3(s) = 0 \tag{61}$$

Substitute (41) and (45) in equation (61) to get equation (62)

$$E_3(s)=\left[\frac{I_2^*(s)\left[s^2(K_{12})+s(K_{13})+(K_{14})\right]+K_{15}sV_g(s)}{\left[s^2(K_9)+s(K_{10})+(K_{11})+K_i\left(\frac{1}{s}\right)\right]}\right] \quad (62)$$

Equation (62) describes the grid current error in the s-domain in case we have SMC and IC together.

4.1.3 Addition Of Multi-Resonant Terms

According to the internal model principle in [12], to eliminate the steady state tracking error for sinusoidal current, there should be a mathematical model which can generate the required reference input. There should be a sinusoidal internal model when the system is AC. So, with a high loop gain for specific orders, the resonant controllers are able to suppress the error in these specific orders.

The resonant terms in this system are:-

$$Kr\left[\frac{s}{s^2+w_0{}^2}\right] \quad (63)$$

Equation (63) corresponds to the resonant term acts on the grid current steady state error at the fundamental frequency trying to eliminate it with a suitable gain Kr

$$Kr\left[\frac{s}{s^2+(nw_0)^2}\right] \quad (64)$$

Equation (63) corresponds to the resonant terms act on the grid current steady state error (SSE) at the higher order frequency components starting from the 3rd harmonic order with the purpose of eliminating SSE with a suitable gain Kr.

At steady state the switching function average value is zero. Then we have:

$$\sigma(s) = c_1 E_1(s) + c_2 E_2(s) + c_3 E_3(s) + K_i \left(\frac{1}{s}\right) E_3(s)$$
$$+ Kr \left[\frac{s}{s^2 + w_0^{\,2}}\right] E_3(s) + Kr \sum_{n=3}^{21} \left[\frac{s}{s^2 + (n w_0)^2}\right] E_3(s) = 0 \quad (65)$$

We take the harmonic orders in the simulation from n=3 until n=21

Substitute (41) and (45) in equation (65) to get equation (66)

$$E_3(s) = \left[\frac{I_2^{\,*}(s)\left[s^2(K_{12}) + s(K_{13}) + (K_{14})\right] + K_{15} s V_g(s)}{\left[s^2(K_9) + s(K_{10}) + (K_{11}) + K_i\left(\frac{1}{s}\right) + Kr\left[\frac{s}{s^2 + w_0^{\,2}}\right] + Kr\sum_{n=3}^{21}\left[\frac{s}{s^2 + (n w_0)^2}\right]\right]}\right] \quad (66)$$

4.2 Theoretical Results

The theoretical results achieved with the given values for the system parameters in table 1 using matlab 2015 in case of SMC alone, (SMC and IC), (SMC, IC, and MRC).

Table 1: The values of the system parameters

Parameters	**Values**
L1	1.2mH
L2	0.4mH
C	50μF
V_{DC}	500V
Vg (r.m.s)/f_0	220V/50Hz
I2	35A
fs	20KHz/33.33KHz
c_1	1
c_2	2
c_3	40
k	$5*10^4$
ε	$8*10^4$
Ki	10^4
Kr	30

4.2.1 SMC Alone

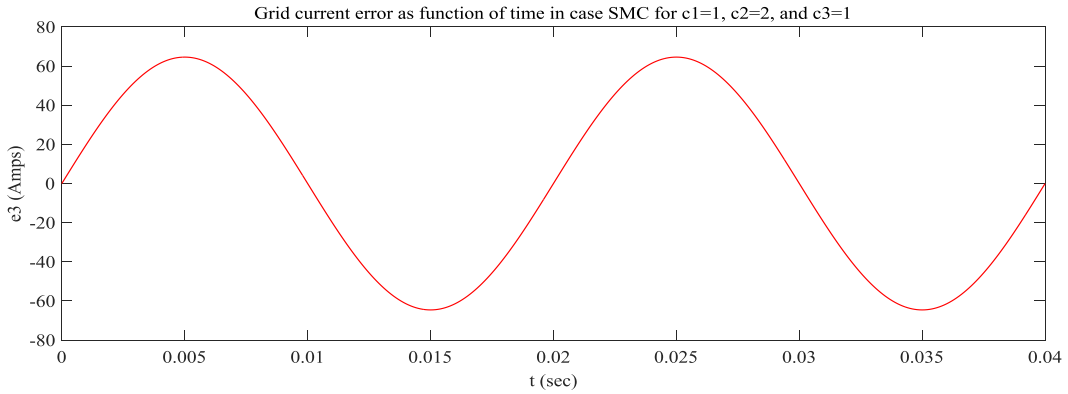

Figure14: Grid current error for as c_3=1 function of time using SMC alone

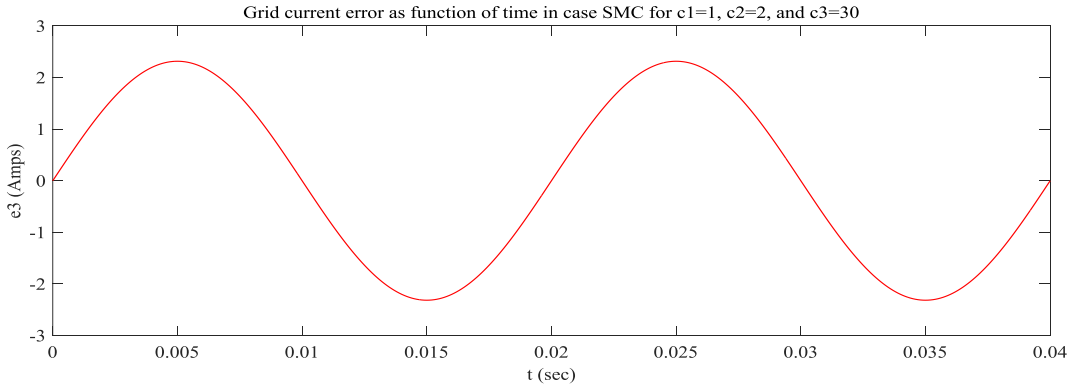

Figure 15: Grid current error for c_3=30 as function of time using SMC alone.

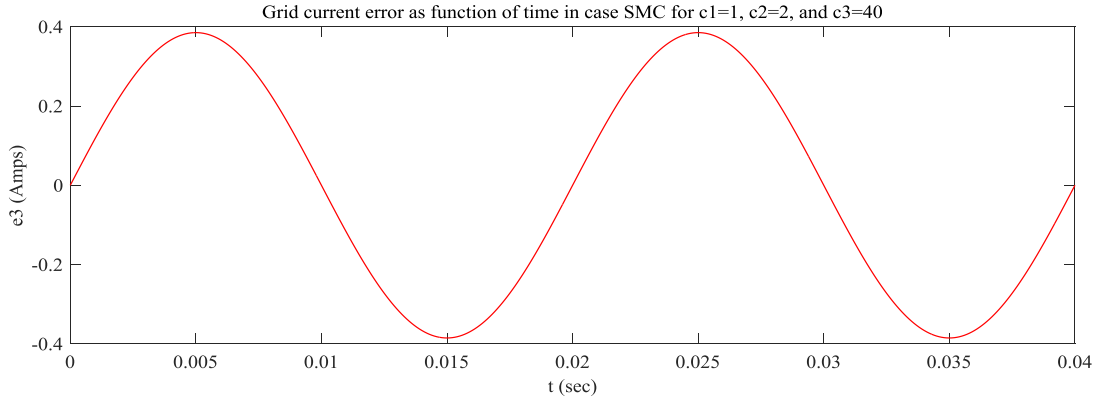

Figure 16: Grid current error for c_3=40 as function of time using SMC alone.

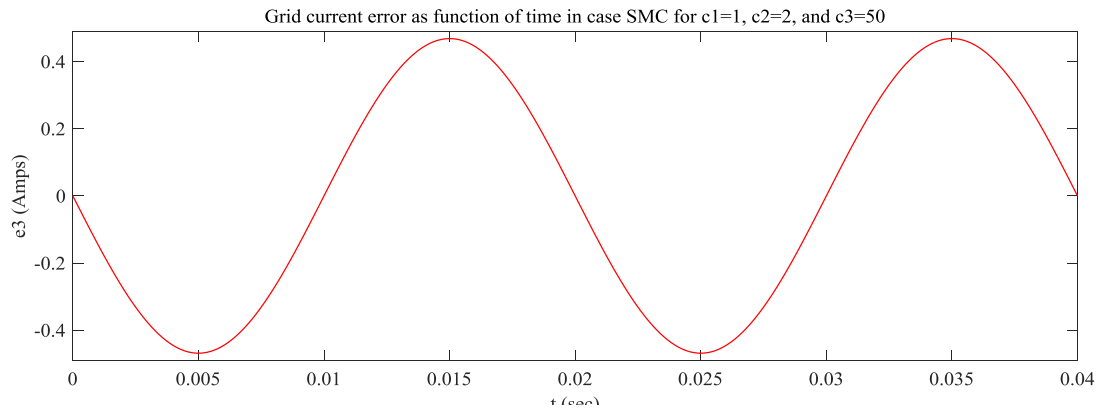

Figure 17: Grid current error for c_3=50 as function of time using SMC alone.

In Figures 14 and 15, the steady state error (SSE) in the grid current is unacceptable. However, for c_1=1, c_2=2 and c_3=40 the steady state error (SSE) decreases to reach 0.4A. In Figure 17, the steady state error (SSE) increases to become more than the previous value which is 0.4A. This proves that the most suitable sliding surface is occurred when c_1=1, c_2=2 and c_3=40. Although, SMC alone cannot eliminate the SSE. So, addition of the integral controller should eliminate the steady state error in the grid current.

4.2.2 SMC With IC

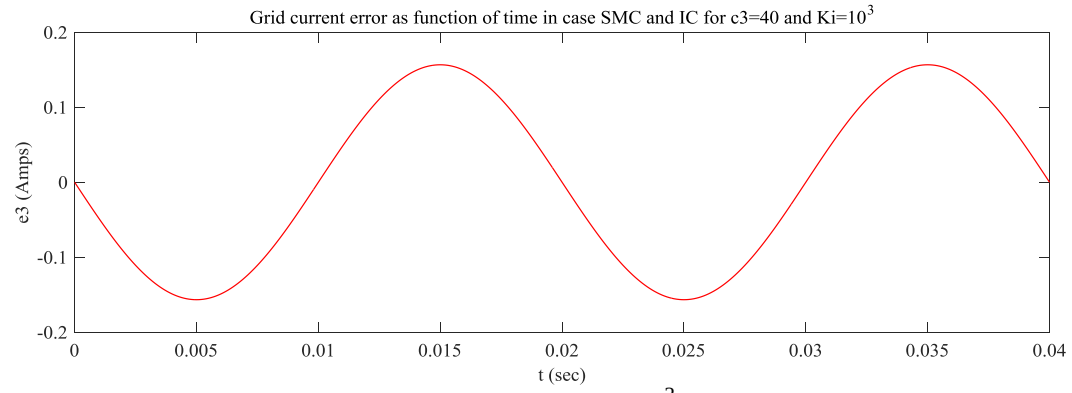

Figure 18: Grid current error for c_3=40 and Ki=10^3 as function of time using SMC and IC.

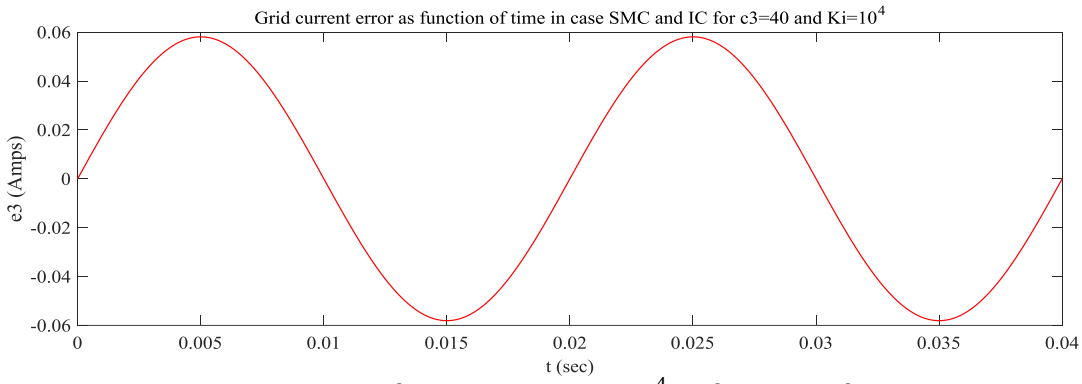

Figure 19: Grid current error for c_3=40 and Ki=10^4 as function of time using SMC and IC.

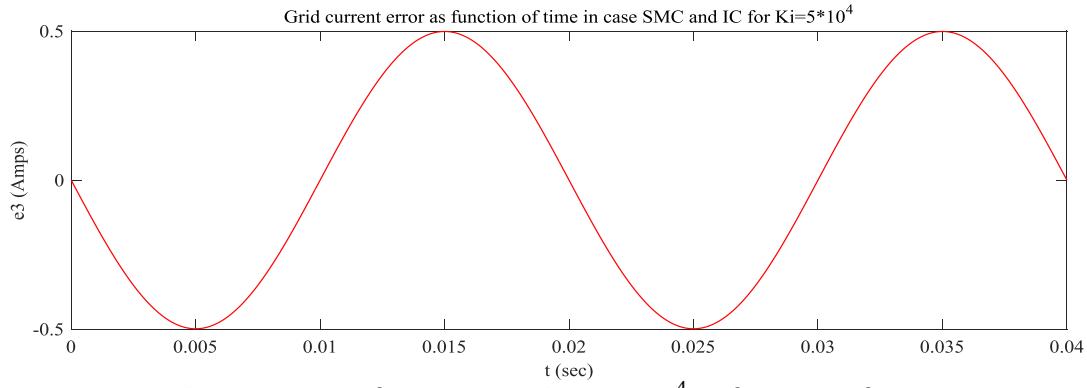

Figure 20: Grid current error for c_3 =40 and Ki=5*10^4 as function of time using SMC and IC.

We conclude that as the integral controller gain increases, the grid current error decreases until Ki=10^4 to reach 0.06A. However, Figure 20 proves that there is a limit for integral controller gain which is not greater than 10^4 because the SSE in grid current increases again when we increase IC gain to Ki=5*10^4. It is obvious that addition of the integral controller with sliding mode controller gives the system the ability to approximately suppressing the sinusoidal tracking error for grid current.

4.2.3 SMC, IC, And MRC

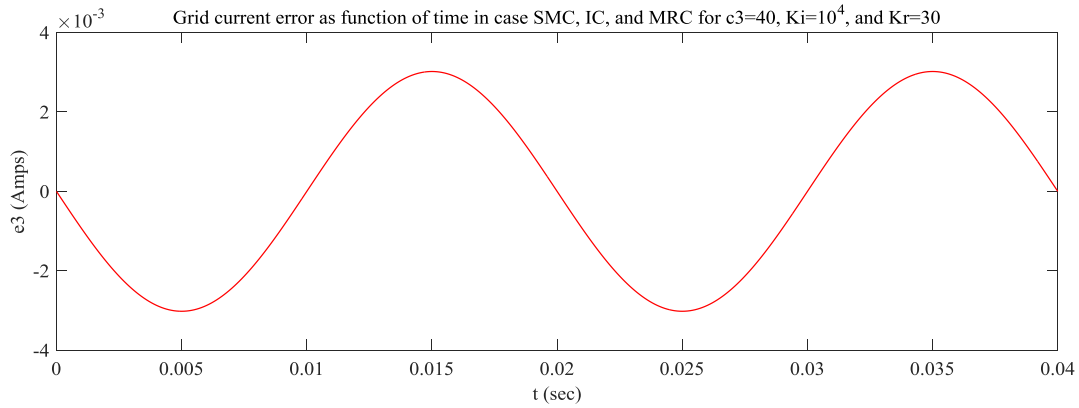

Figure 21: Grid current error as function of time in case of SMC, IC, and MRC for Kr=30 and $Ki=10^4$

We conclude that adding the resonant terms from n=1 until n=21 to SMC and IC suppresses the grid current error until reach $3*10^{-3}$ A. The reason behind that is the high loop gain at special order frequencies as stated in [12].

Chapter 5

THE PROPOSED MODEL AND SIMULATION

5.1 The Proposed Model For The Whole System

The implementation of the model for the whole system with sliding mode controller (SMC), integral controller (IC), and multi-resonant controller (MRC) using mat-lab Simulink 2015 is shown in this chapter.

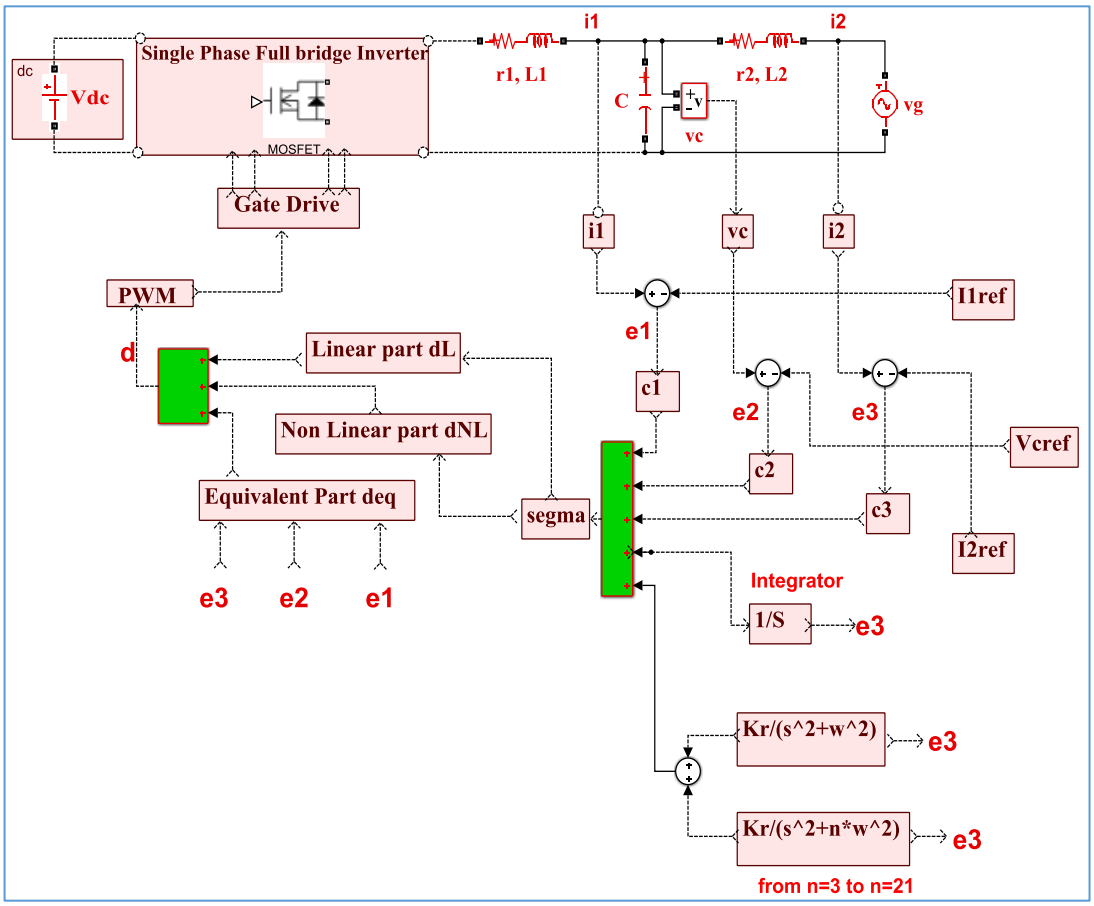

Figure 22: Grid current control for single phase inverter with LCL filter using SMC, IC, and MRC.

Before introducing the model of the system, Figure 22 can show the control diagram for single phase VSI with LCL filter under the proposed control strategy. This Figure gives the reader the ability to understand generally how the model works.

During implementation of the proposed model of the system, each part is designed alone and implemented in sub-block and defined by its name. After dividing the proposed model into many sub-blocks, we connect all these sub-blocks together in a very careful manner to construct the whole controller. We use the measurement devices available in the Simulink to measure and plot all the required outputs of the system. After that, the results are simulated.

Each sub-block that represents a specific part of the controller will be shown. But first of the all, the propose model for the whole system is shown in Figure 23.

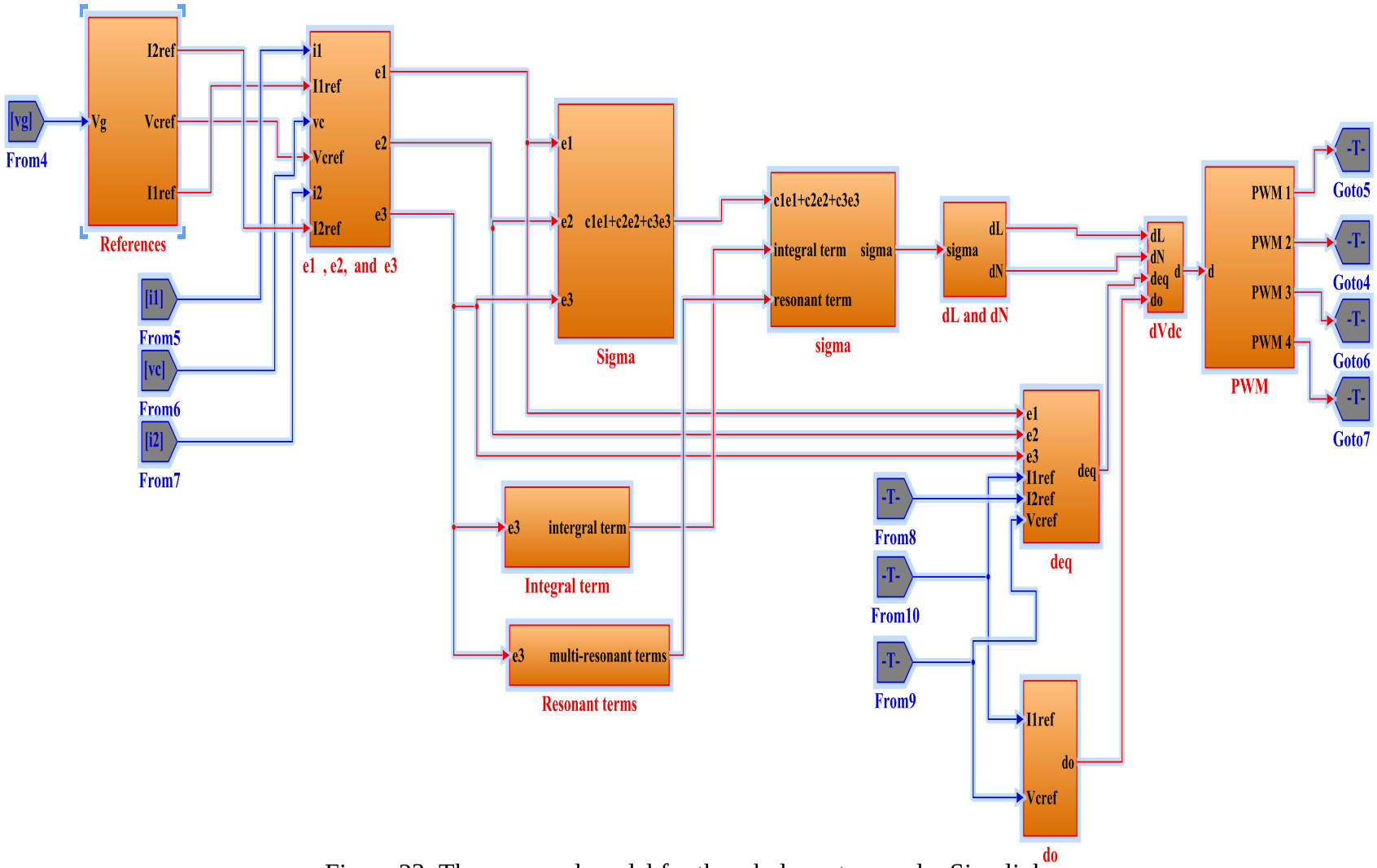

Figure 23: The proposed model for the whole system under Simulink.

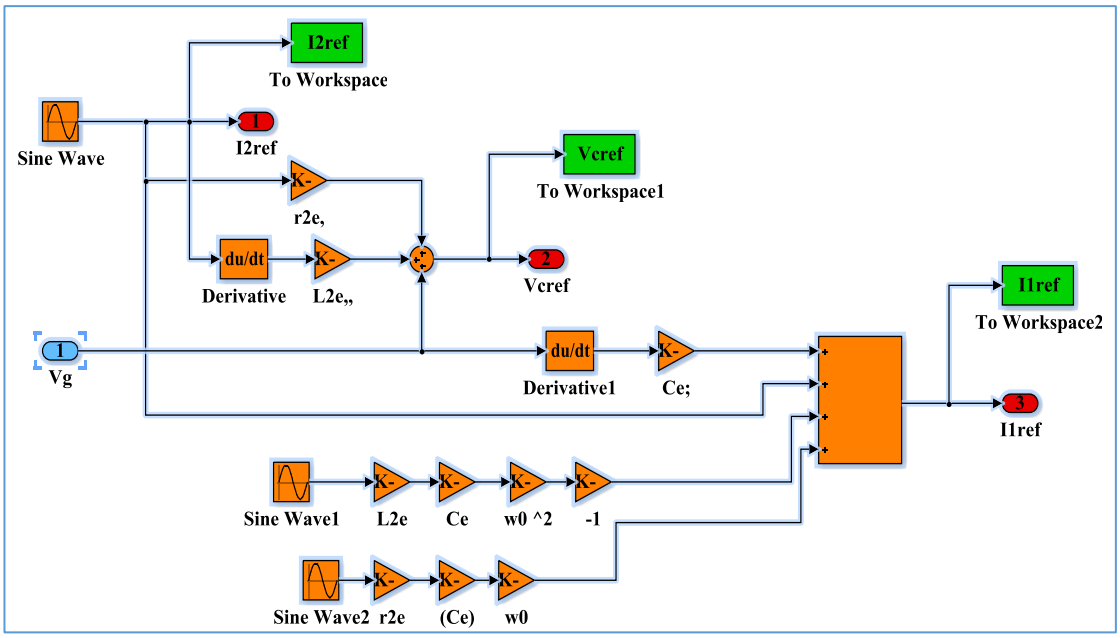

Figure 24: Reference Functions in the system that are defined in Chapter 2.

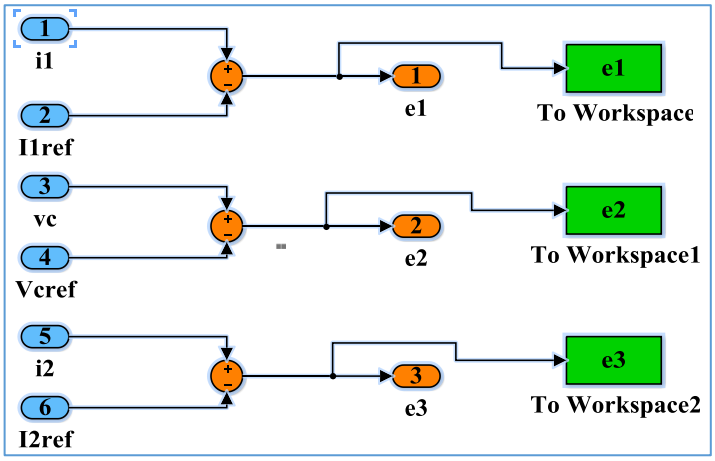

Figure 25: Errors in system that are defined in Chapter 2.

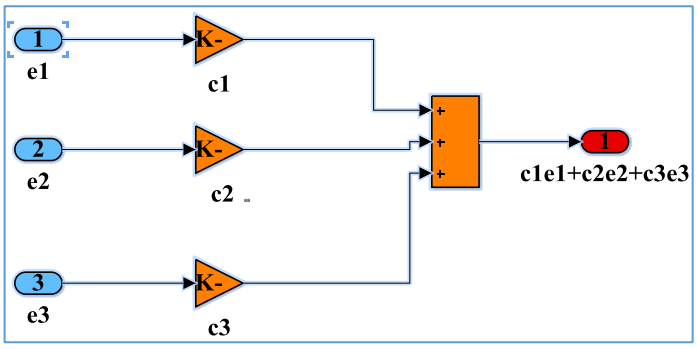

Figure 26: Switching function of the system that is defined in Chapter 3.

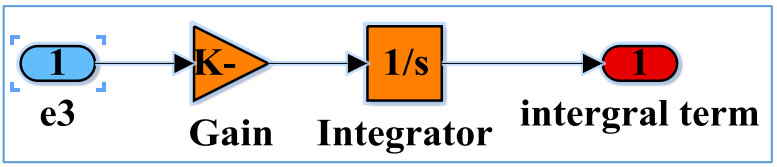

Figure 27: Integral controller that is defined in Chapter 4.

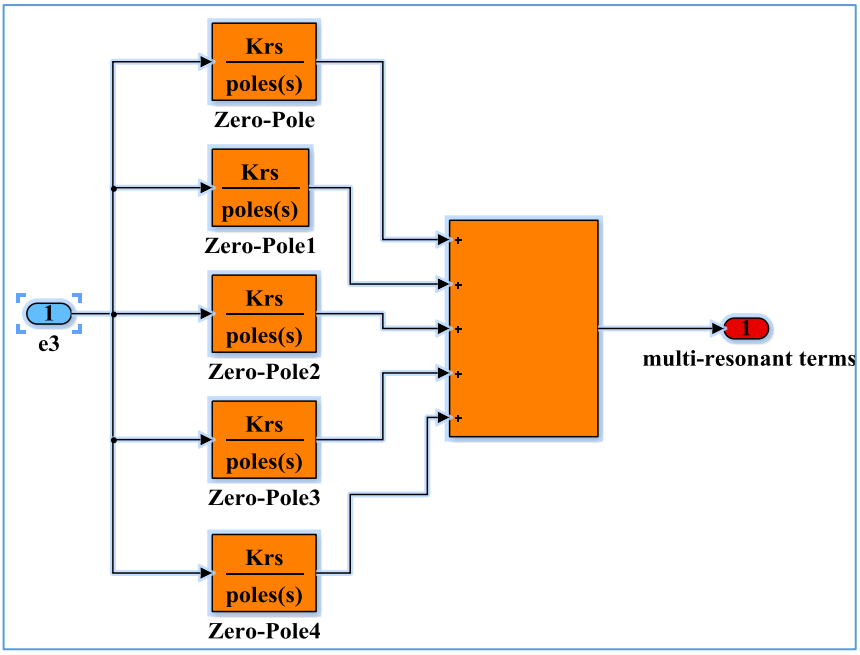

Figure 28: Five Multi-resonant terms used in the Simulink matlab that are defined in Chapter 4.

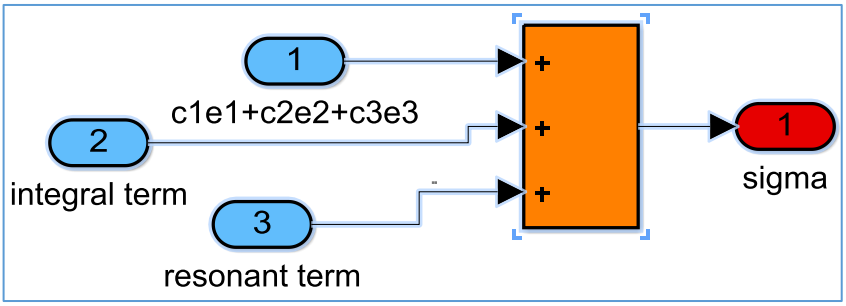

Figure 29: Switching function with combination of all controllers include SMC, IC, and MRC as defined in Chapter 4.

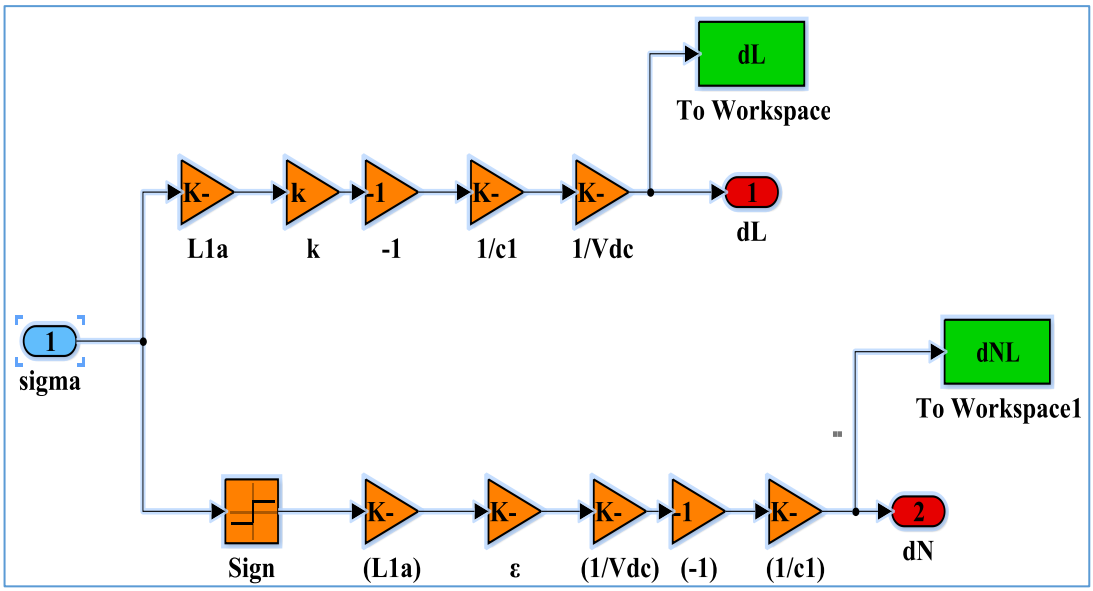

Figure 30: Linear and non-linear parts of the control input as defined in Chapter 3.

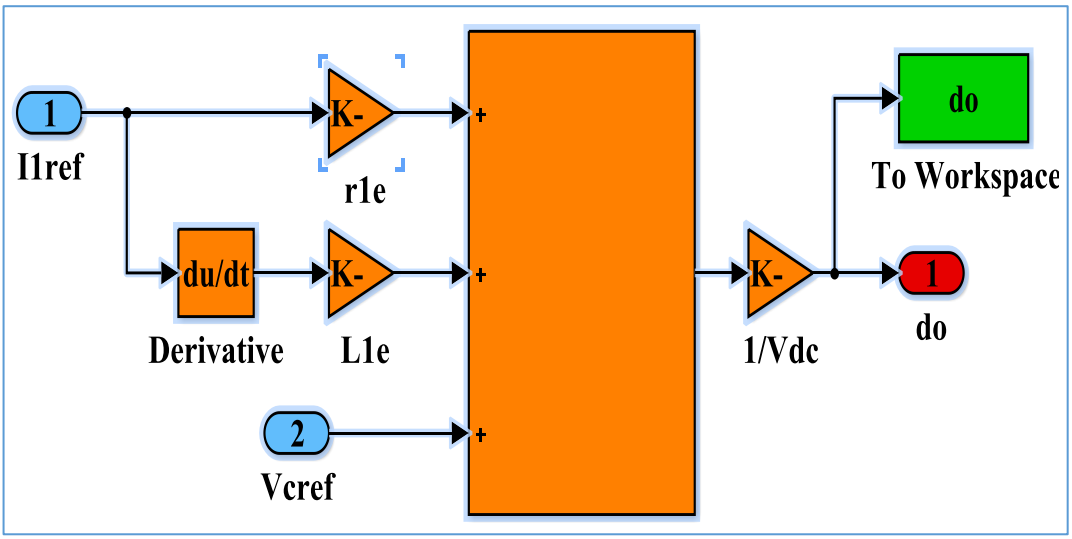

Figure 31: Control input at steady state as defined in Chapter 2.

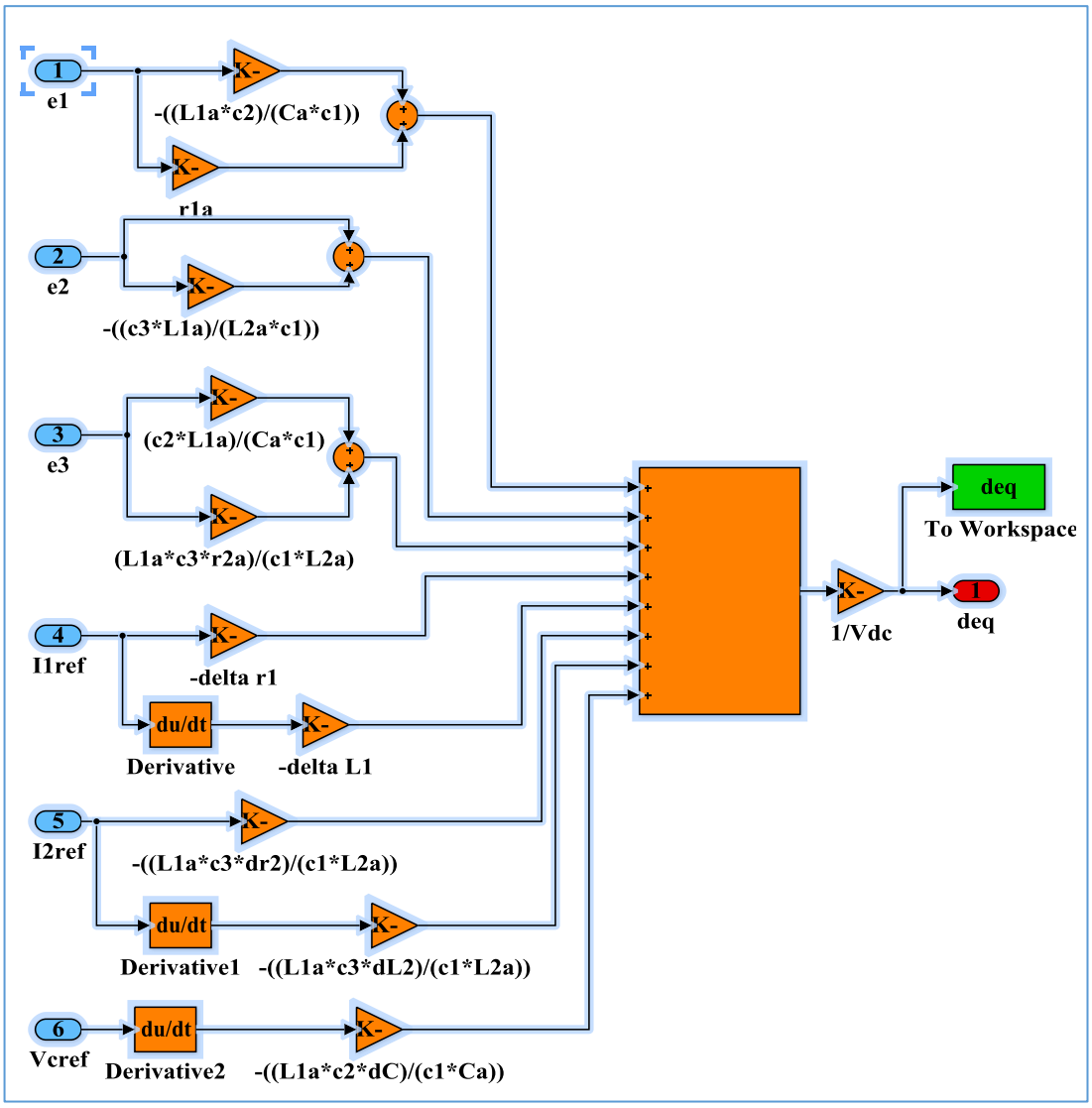

Figure 32: Equivalent part of the control input as defined in Chapter 3.

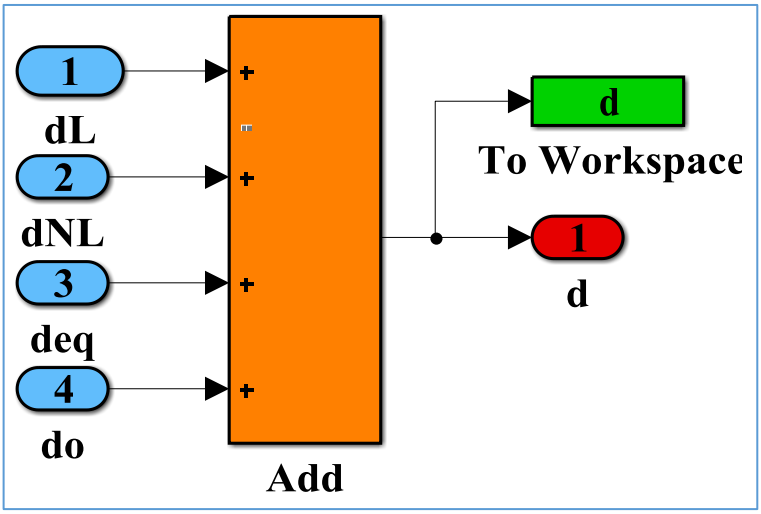

Figure 33: Total control input of the system as defined in Chapter 3.

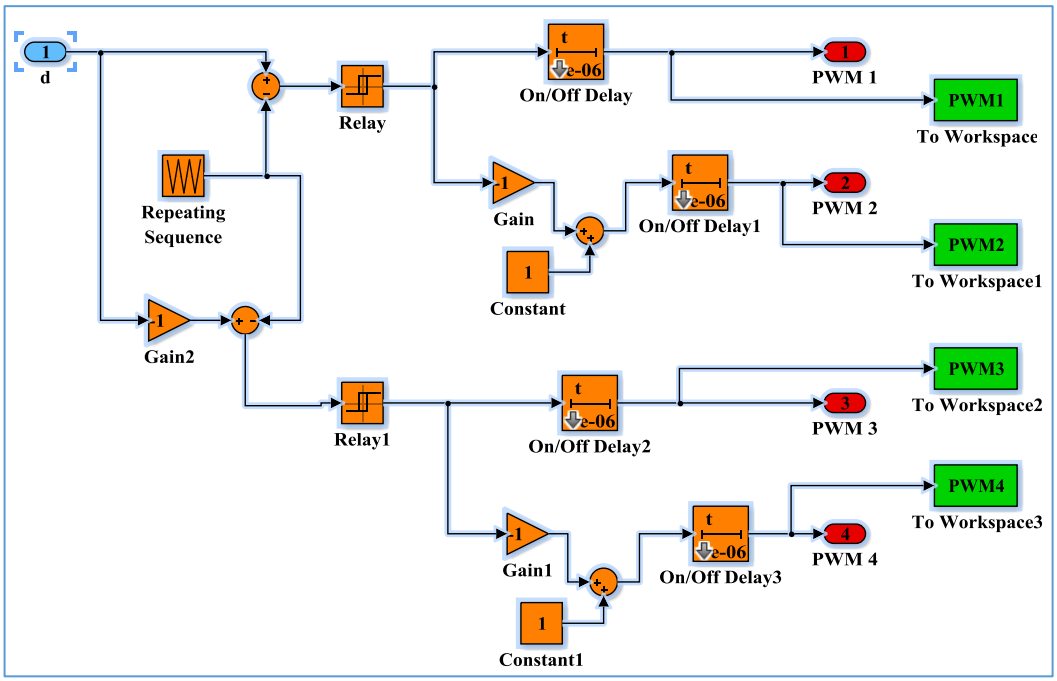

Figure 34: PWM technique that is responsible for giving pulses to the switches.

5.2 Simulation Results

The simulated results on matlab Simulink 2015 for the grid current error, grid current, and reference currents and voltages in case of SMC, (SMC and MRC) ,(SMC and IC), and (SMC, IC, and MRC) is shown. During the simulation, we insert an external disturbances in the system including the change in the value of grid reference current between 25A and 35A. Also, another disturbance is changing the value of grid voltage within 10% and insertion of 3^{rd} and 5^{th} harmonics into the grid voltage (V_{3g}=40v and V_{5g}=20v). The variation in the value of the parameters of the LC filter is considered 25% from estimated value.

5.2.1 SMC Alone

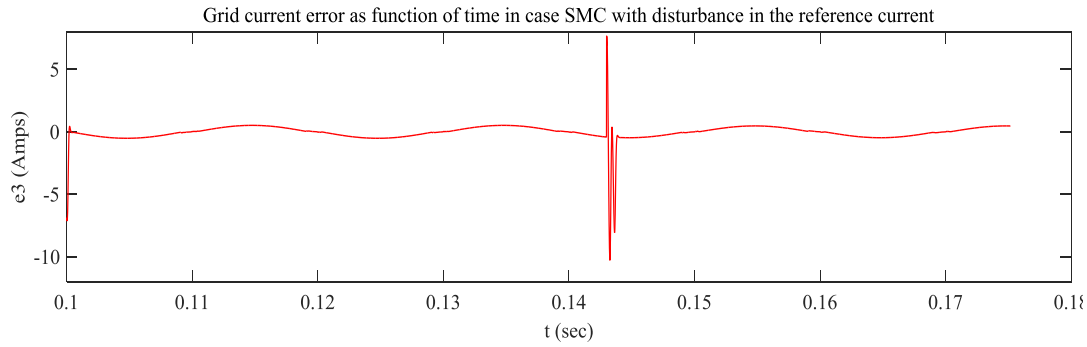

Figure 35: Grid current error as function of time in case SMC for c_3=40 with applied disturbance by decreasing the grid reference current from 35A to 25A.

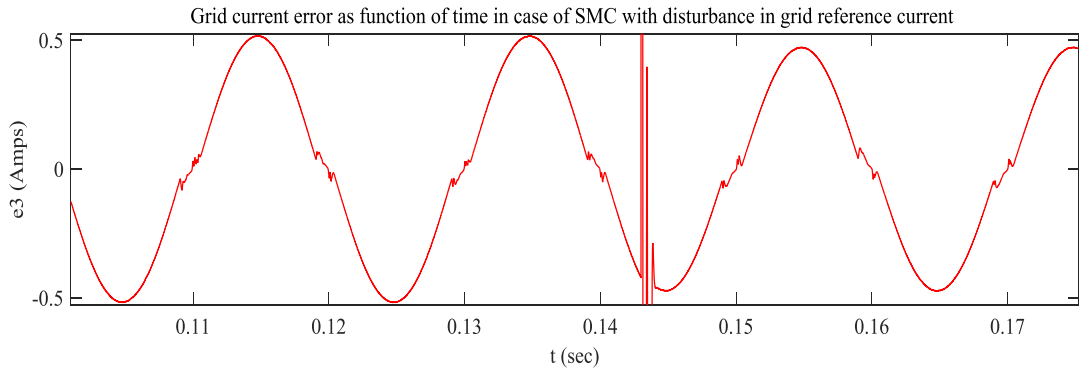

Figure 36: Grid current error as function of time in case SMC with applied disturbance by decreasing the grid reference current from 35A to 25A after zooming the previous Figure.

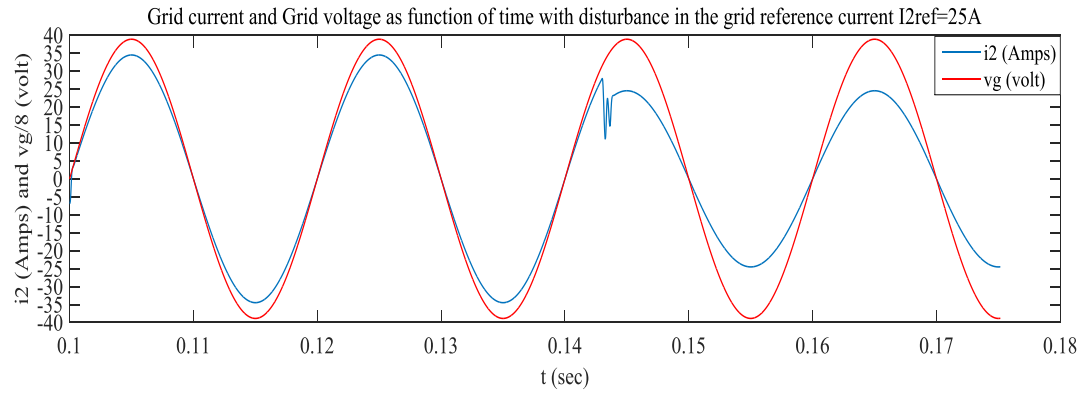

Figure 37: Grid current and grid voltage as function of time in case SMC with applied disturbance by decreasing the grid reference current from 35A to 25A.

We conclude that sliding mode controller SMC decreases the magnitude of the grid current error for c_1=1, c_2=2, and c_3=40 to 0.5A as shown in Figure 36. In the field of

disturbance injection and rejection, we decrease I2ref from 35A to 25A after time=0.14sec as an external disturbance in the system but SMC rejects this disturbance and the grid current continues its pure sinusoidal wave form as seen in figure 37 and the system stability survived.

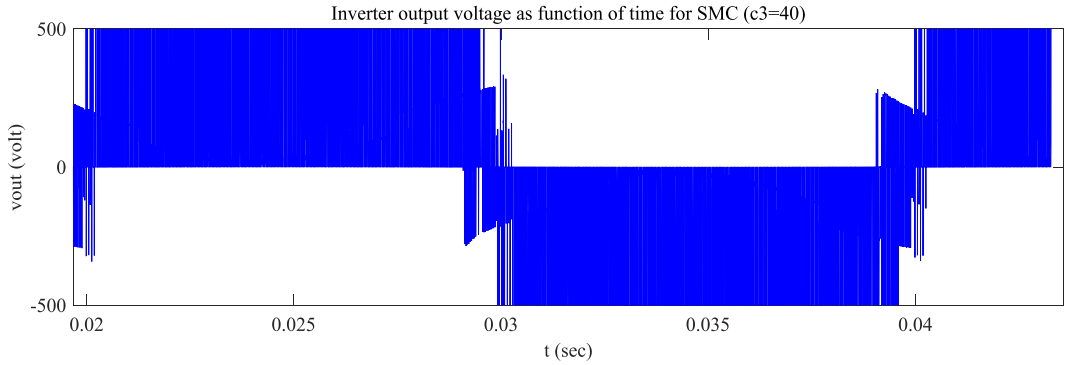

Figure 38: Inverter output voltage as function of time using SMC controller alone.

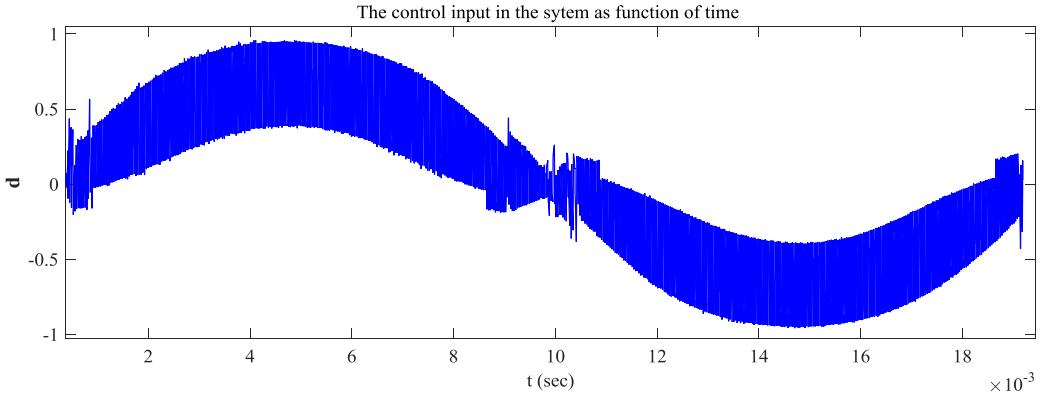

Figure 39: Control input of the system as function of time using SMC.

The inverter output voltage is a square waveform as in Figure 38. The control input of the system shown in Figure 39 is a sinusoidal waveform with a high switching frequency. This control input has a variable switching frequency approximately in range between 20 KHz and 33.33 KHz. This is the main disadvantage of the sliding mode control because variable switching frequency causes heating and oscillations in the system. This results in a system with high losses and less stability.

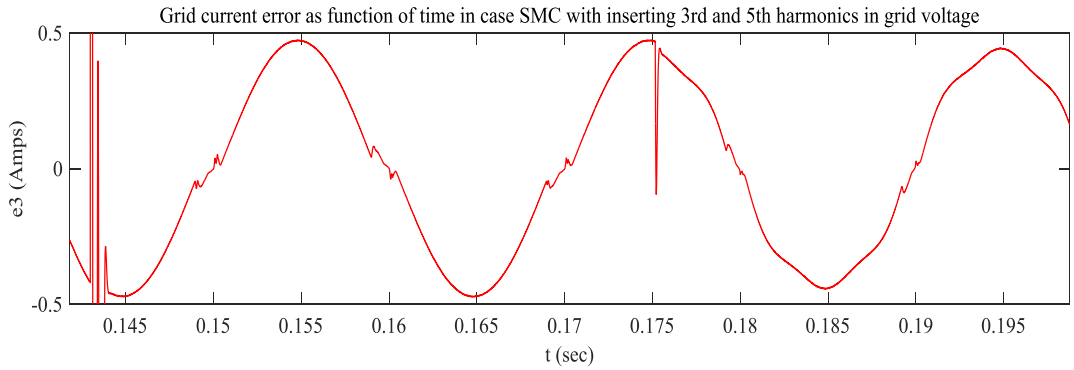

Figure 40: Grid current error as function of time in case SMC for c_3=40 with inserting 3rd and 5th harmonics in grid voltage at t=0.175sec.

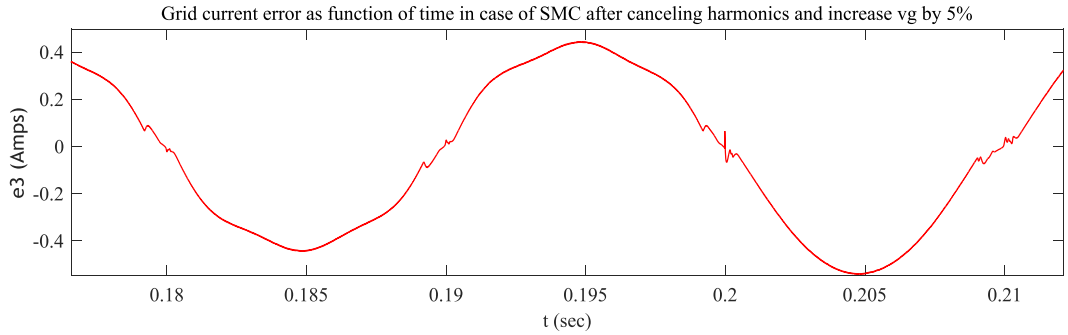

Figure 41: Grid current error as function of time in case SMC for c_3=40 after deleting harmonics in grid voltage and increase the amplitude of grid voltage by 5% to reach 327volt at t=0.2sec.

We conclude that the Second disturbance which is the injection of the 3rd and 5th harmonics (V_{3g}=40v and V_{5g}=20v) into the grid voltage at time =0.175sec is rejected by the sliding mode controller and the wave forms of the grid current error continue its normal wave form with slightly small harmonics in its contents as shown in Figure 40. After that, we suppose changes have occurred in the grid voltage by deleting the harmonics contents and increasing grid voltage amplitude 5% to reach 327v at time=0.2 sec as shown in Figure 41 but again SMC rejects this disturbance and the stability of the system survived.

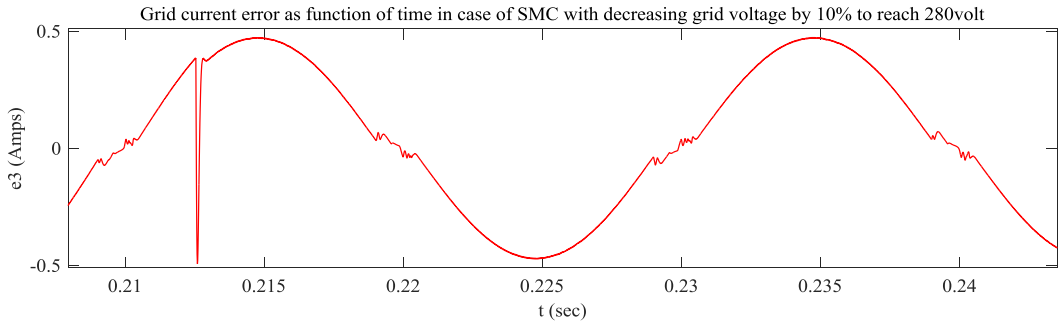

Figure 42: Grid current error as function of time in case SMC for c_3=40 with decreasing the grid voltage amplitude by 10% to reach 280volt.

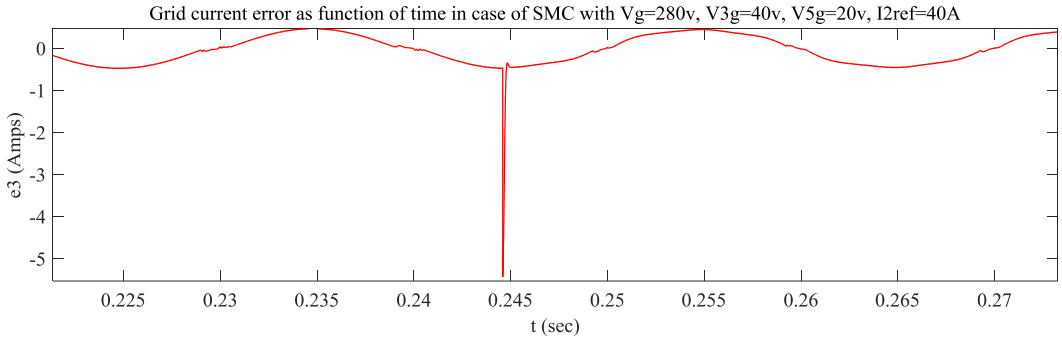

Figure 43: Grid current error as function of time in case SMC for c_3=40 with decreasing grid voltage amplitude by 10% to reach 280volt with inserting 3rd and 5th harmonics in grid voltage and also increase reference grid current from 35A to 40A.

Also, another disturbance is decreasing the amplitude of the grid voltage by 10% to reach 280v at time=0.213sec as shown in Figure 42 but again SMC rejects this disturbance and the system stability survived. After that, at time=0.242sec as shown in figure 43 we insert disturbances with decreasing grid voltage amplitude by 10% with inserting 3rd and 5th harmonics in grid voltage and also increase reference grid current from 35A to 40A. But again SMC rejects all these different disturbances that occurred at the same time and the system stability again survived.

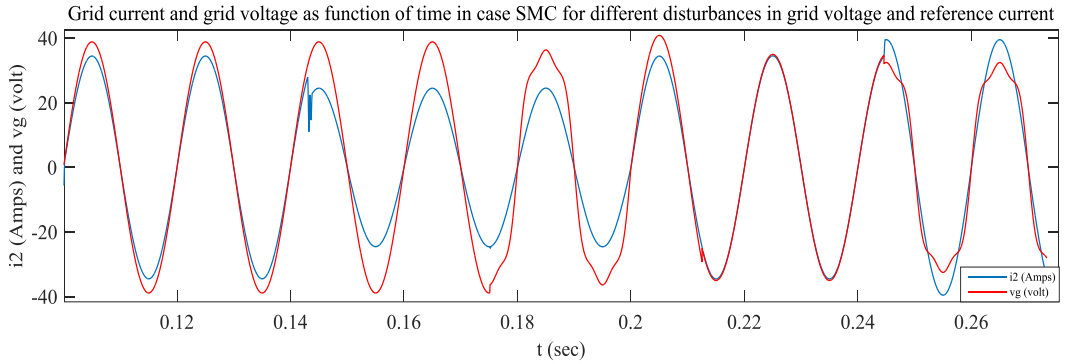

Figure 44: Grid current and grid voltage as function of time in case SMC for c_3=40 with different disturbances in grid reference current and grid voltage.

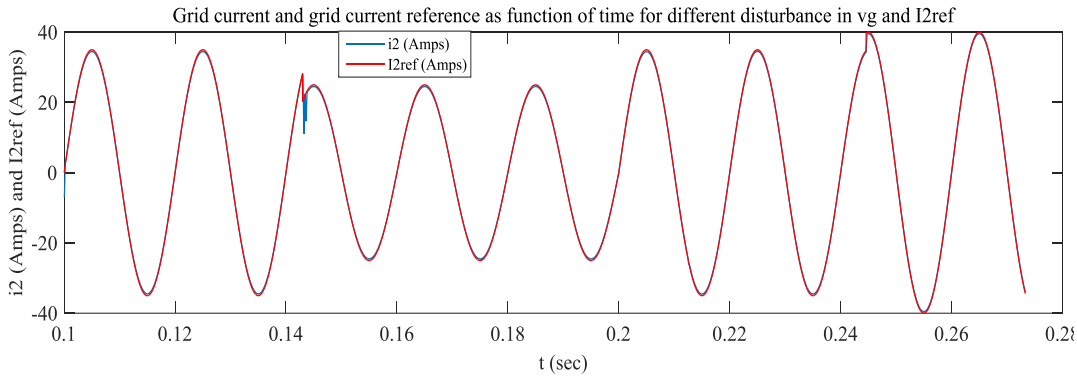

Figure 45: Grid current and grid current reference as function of time in case SMC for c_3=40 with difference disturbances in grid voltage and grid current reference.

From figure 44 and 45, we conclude that the SMC rejects all disturbances that can occur in the grid voltage or grid reference current. We see from figure 44 that grid current and grid voltage are in phase and from figure 45 we see that grid current always tracks its reference.

We conclude that SMC can rejects any disturbances in the grid voltage, grid reference current, and filter parameters but alone it cannot suppress the steady state error (SSE) in the grid current.

5.2.2 SMC With MRC

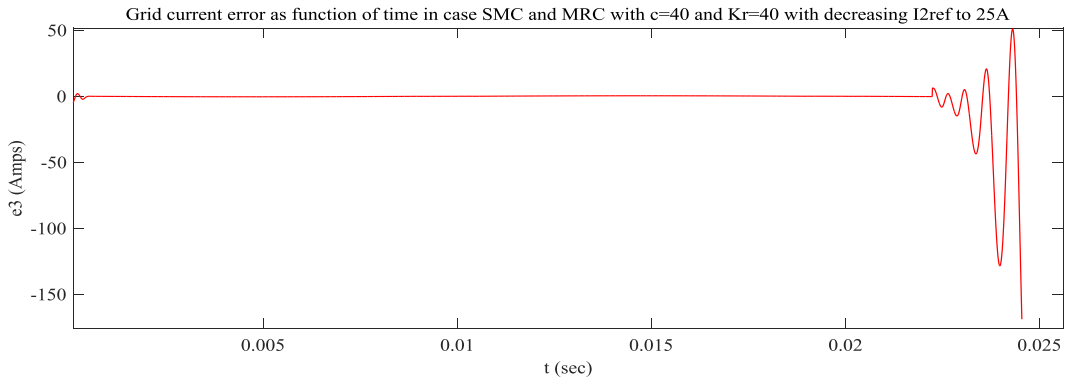

Figure 46: Grid current error as function of time in case SMC and MRC for c_3=40 and Kr=40 with disturbance for decreasing I2ref from 35A to 25A.

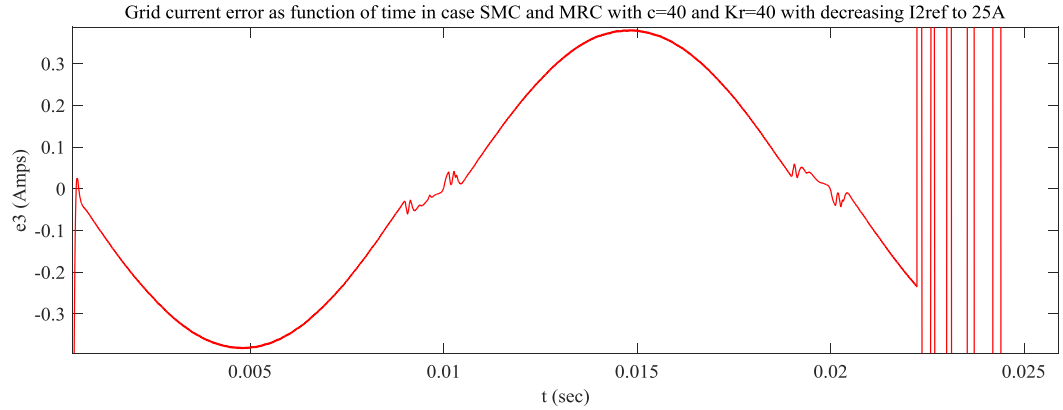

Figure 47: Grid current error as function of time in case SMC and MRC for c3=40 and Kr=40 after insertion decreasing I2ref from 35A to 25A.

We add MRC with SMC for Kr =40 and we insert disturbance by decreasing I2ref from 35A to 25A at time t=0.022sec. The system becomes unstable as seen in Figure 46. After zooming Figure 46 to get Figure 47, we notice that for Kr=40 the magnitude of the grid current error decreases from 0.5A to reach 0.4A.

We conclude that for Kr $\geq$ 40, the grid current error magnitude decreases. However, with disturbance MRC cancel the effective behavior of SMC in rejection of the disturbance and the system becomes unstable.

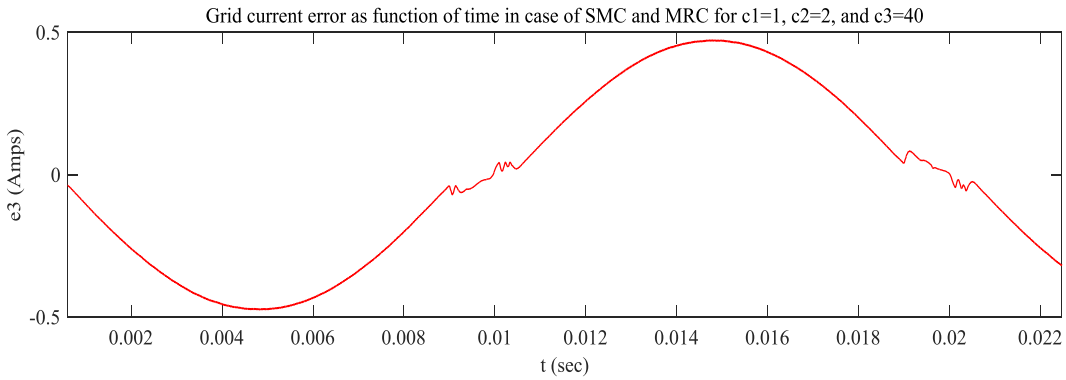

Figure 48: Grid current error as function of time in case SMC and MRC for c3=40 and Kr=30.

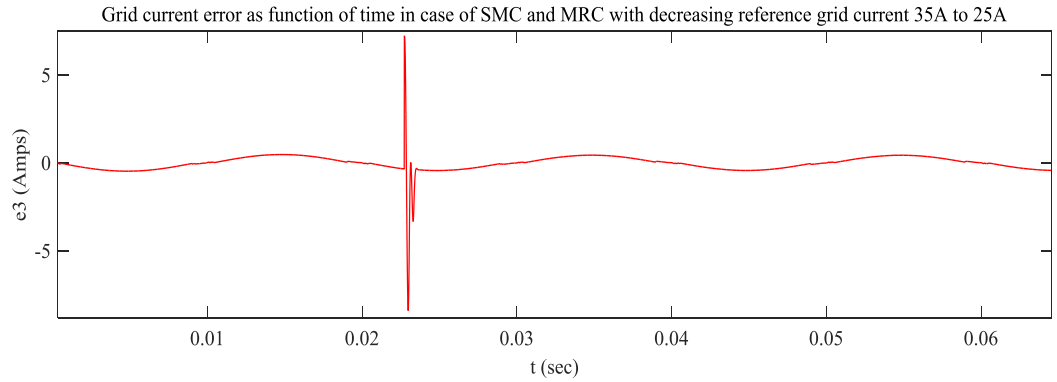

Figure 49: Grid current error as function of time in case SMC and MRC with disturbance for decreasing the grid reference current from 35A to 25A.

We conclude that for Kr≤ 30, the magnitude of the grid current error decreases from 0.5A to reach 0.48A as seen from Figure 48 which is very small effect but this value for the gain of MRC, the disturbance for decreasing I2ref to 25A is rejected as shown in Figure 49 and the system survived and stayed stable.

We conclude that a high value of gain for MRC decreases the grid current error but makes the system unstable for any external disturbance on the system.

5.2.3 SMC With IC

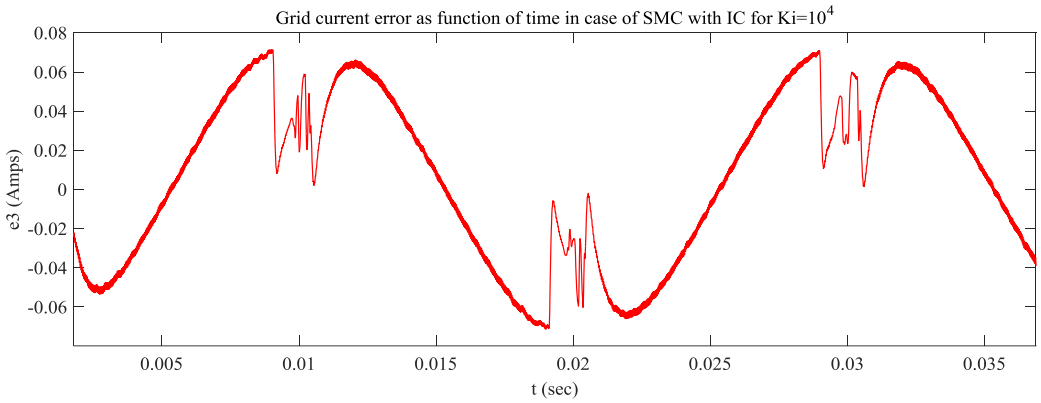

Figure 50: Grid current error as function of time in case of SMC and IC for Ki=10^4.

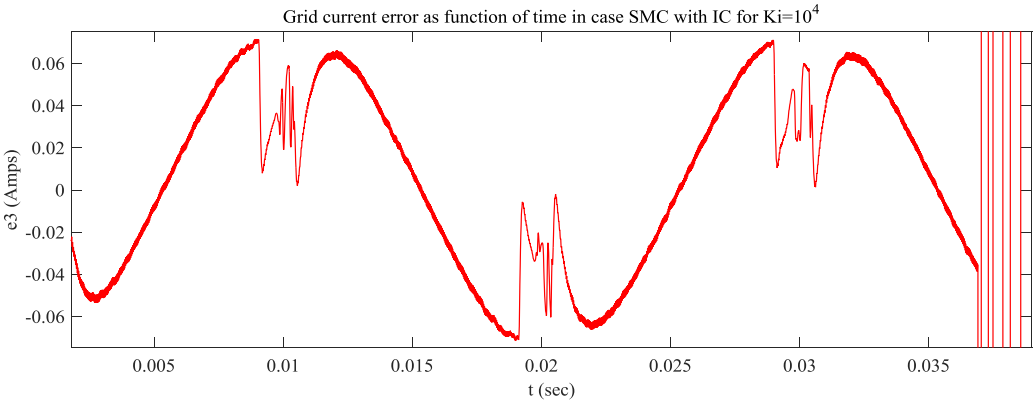

Figure 51: Grid current error as function of time in case of SMC and IC for Ki=10^4 after decreasing I2ref from 35A to 25A.

SMC with IC is very powerful control strategy for decreasing the magnitude of the grid current error as shown in figure 50 which the grid current error decreases from 0.5A to reach 0.07A. After inserting a disturbance by decreasing I2ref from 35A to 25A, the system becomes unstable as shown in figure 51.

We conclude that integral controller with SMC can't achieve the stability of the system with an external disturbance.

5.2.4 All Controllers (SMC, IC, MRC)

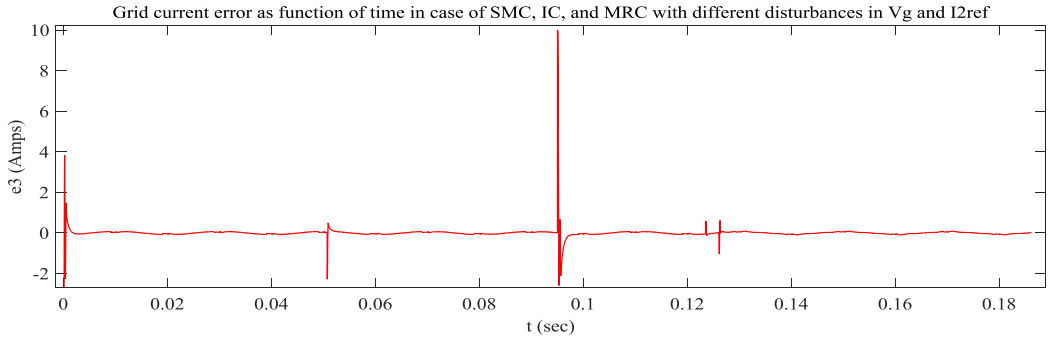

Figure 52: Grid current error as function of time in case of SMC, IC, and MRC for Ki=10^4 and Kr=30 for different disturbances occurred in grid voltage and grid reference current.

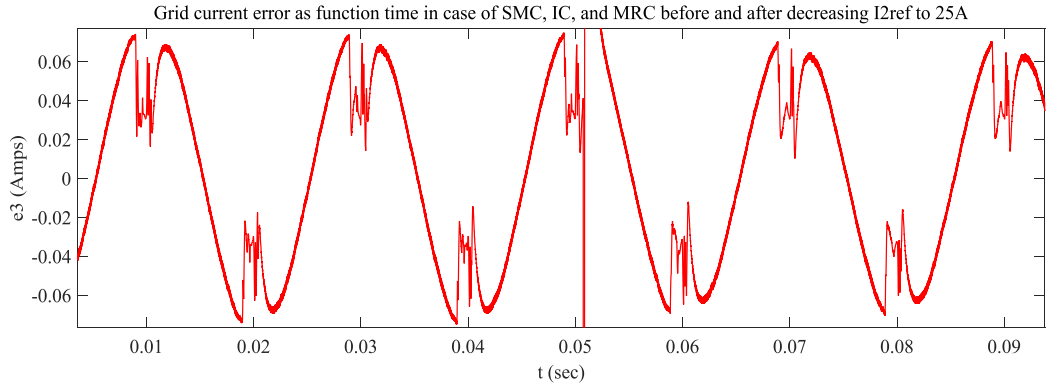

Figure 53: Grid current error as function of time in case of SMC, IC, and MRC for Ki=10^4 and Kr=30 after decreasing I2ref from 35A to 25A.

We combine SMC, IC, and MRC all together to study their effect on the dynamic behavior of the system. We insert different disturbances in the grid voltage and grid reference current as shown in Figure 52. SMC and IC couldn't reject the disturbances but after adding MRC the system remains stable by rejecting all the applied disturbances. We conclude that MRC for small gain helped IC to decrease the grid current error with achieving the stability by rejecting all the applied external disturbances. Zooming Figure 52 to get Figure 53 which shows how the system rejects the applied disturbance at time =0.05sec and remained stable.

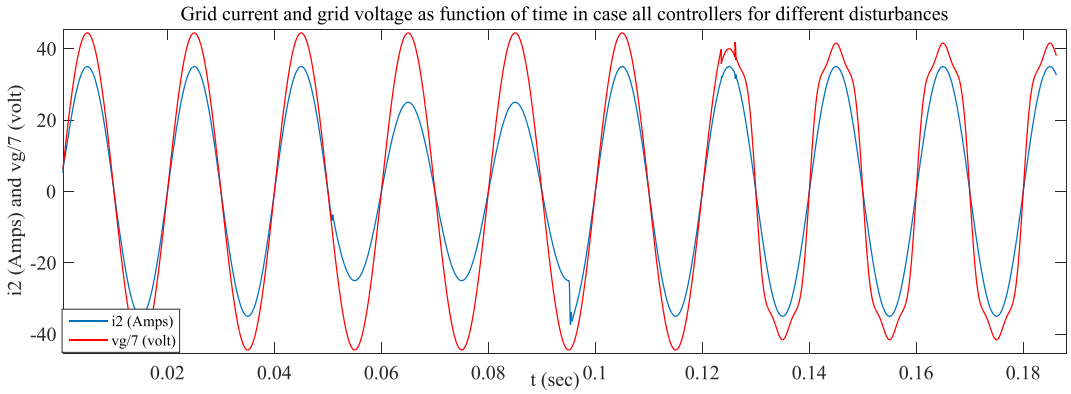

Figure 54: Grid current and grid voltage (scaled by 1/7) as function of time in case of SMC, IC, and MRC for Ki=10^4 and Kr=30 for different disturbances occurred in grid voltage and grid reference current.

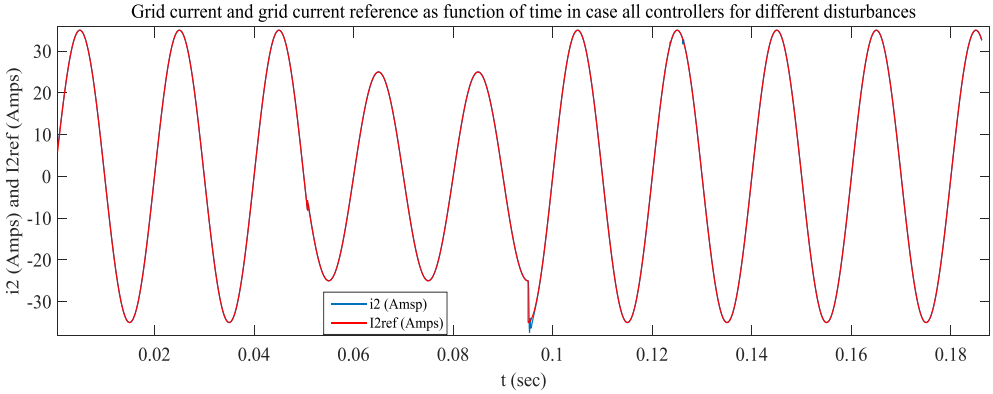

Figure 55: grid current and grid current reference as function of time in case of SMC, IC, and MRC for Ki=10^4 and Kr=30 for different disturbances occurred in grid voltage and grid reference current.

We conclude that the combination of all these controllers give the system the ability to rejects all disturbances that can occur in the grid voltage or grid reference current. We see from Figure 54 that grid current and grid voltage are in phase and from Figure 55 we see that grid current always tracks its reference.

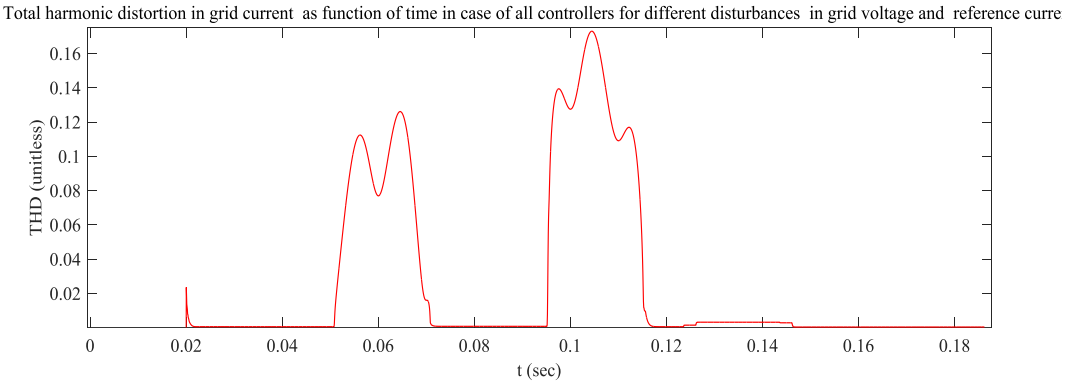

Figure 56: Total harmonic distortion in grid current as function of time in case of SMC, IC, and MRC for Ki=10^4 and Kr=30 for different disturbances occurred in grid Voltage and grid reference current.

Figure 56 explains the variations occurred in the total harmonic distortion in the grid current for different disturbances in the system. %THD of the system is 0.05% which is approximately negligible and this proves the effectiveness of the applied control strategy on the total harmonics distortion in the system.

5.3 Comparison Between This Thesis And The IEEE Transaction Paper in [11]

Table 2: Similarities in the parameters of the model used in this thesis and the other one in the IEEE transaction paper in [11]

Parameters	**IEEE Transaction Paper in [11]**	**Thesis**
L1	0.4mH	1.2mH
L2	1.2mH	0.4mH
C	50µF	50µF
VDC	500V	500V
Vg (r.m.s)/f0	220V/50Hz	220V/50Hz
I2	35A	35A
fs	15KHz	20KHz/33.33KHz

Table 3: Differences in the parameters of the model used in this thesis and the other one in the IEEE transaction paper in [11]

Parameters	**IEEE Transaction Paper in [11]**	**Thesis**
c1	1	1
c2	1	2
c3	1	40
k	$2.0833*10^4$	$5*10^4$
ε	$4.1667*10^4$	$8*10^4$
Ki	10^3	10^4
Kr	20	30

Table 4: Comparison in the magnitude of error and THD in four different controllers in this thesis and with that in the IEEE transaction paper in [11].

Cases	**Parameters**	**Results**	
		IEEE Transaction paper in [11]	**Thesis**
SMC	Magnitude of grid current error <e3>	1.25A	0.5A
	%THD (no disturbance)	2.12	0.1367
	%THD (with disturbance)	Not reported	0.1367
SMC+MRC	Magnitude of grid current error <e3>	Not reported	0.48A
	%THD (no disturbance)	Not reported	0.13
	%THD (with disturbance)	Not reported	0.13
SMC+IC	Magnitude of grid current error <e3>	0.65A	0.07A
	%THD (no disturbance)	1.86	0.092
	%THD (with disturbance)	Not reported	0.092
SMC+IC+MRC	Magnitude of grid current error <e3>	$2*10^{-242}$	0.07A
	%THD (no disturbance)	0.91	0.05
	%THD (with disturbance)	0.91	0.05

Chapter 6

CONCLUSION AND FUTURE WORK

6.1 Conclusion

The proposed control strategy in this thesis is the sliding mode controller (SMC) for a single phase grid connected inverter with LCL filter. SMC is a very powerful control strategy in rejecting the external disturbances that can suddenly applied on the system. SMC decreases the grid current error to reach 0.5A, the total harmonic distortion (THD) in the grid current to 0.1367%, and rejects all the applied disturbances in the grid voltage and grid current reference. However, SMC alone couldn't suppress totally the grid current error. An additional integral term decreases the grid current error from 0.5A to reach 0.07A but it couldn't withstand the applied disturbances in the system. Multi-resonant terms have the ability to achieve the stability in the system due to the high loop gain at special frequency orders. Adding MRC to SMC and IC forced the system to withstand any external disturbance in the grid voltage or grid reference current.

So, the Combinations of SMC, IC, and MRC achieve a system with better dynamic response, conserve the stability of the system, robust in rejection the applied disturbances, very small tracking error 0.07A, suppressing the THD in the grid current to reach 0.05%, and make the system reliable.

6.2 Future Work

Sliding mode control strategy main drawbacks in this thesis are the zero crossing disturbances, inverter current reference generation, and the variable switching frequency. In the future, using a new function other than the sign function that has no abrupt change during crossing the sliding surface like the hysteresis approach. This can reduce the zero crossing disturbances. Also, the generation of the inverter output current reference is hard to achieve without any errors due to the presence of the second order derivative. Proportional resonant approach can be used in the future to generate the output inverter current reference without errors. These two additional future approaches can improve the total dynamic behavior of the system.

The adjusted model will be simulated using Simulink matlab and will be proved experimentally.

Another future work is to control the variable switching frequency using a new approach. This new approach will be discussed in a research alone later.

REFERENCES

[1] Parikshith, B. C. (2009). Integrated approach to filter design for grid connected power converters. Indian Institute of Science Bangalore-560 012 India.

[2] Khajehoddin, S. A., & Gao, E. A. (2014). High quality output current control for single phase grid-connected inverters. IEEE Applied Power Electronics Conference and Exposition-APEC 2014. IEEE.

[3] Paice, A., & Derek, A. (1996). *Power electronic converter harmonics*. IEEE press.

[4] Chary, T. B., & Bhagwan, R. J. (2015). LCL Filter Design and Performance Analysis for Grid-Interconnected Systems. *International journal of advanced technology and innovative research*, 7.11:2348-2370.

[5] Erickson, J., Robert, W., & Dragan, M. (2007). Fundamentals of power electronics. Springer Science & Business Media.

[6] Cortés, Patricio, et al. (2008). Predictive control in power electronics and drives. IEEE Transactions on industrial electronics 55.12 : 4312-4324.

[7] Vodovozov, A., Valery. R., & Raik, J. (2006). *Power electronic converters*. Tallinn University of Technology Department of Electrical Drives and Power Electronics.

[8] Ekanayake, M., Janaka, F., & Gao, A. (2006). *Power Electronic Converters*. Smart Grid: Technology and Applications: 187-203.

[9] Vadim, I. U. (1977). Survey paper variable structure systems with sliding modes. IEEE Transactions on Automatic control, 22.2 : 212-222.

[10] Bartoszewicz, M., Andrzej, B., & Ron J. P. (2007). Sliding mode control. *International Journal of Adaptive Control and Signal Processing*, 21.89: 635-637.

[11] Hao, X., Chen, W., Huange, L., & Liu, T. (2013). A sliding-mode controller with multi-resonant sliding surface for single-phase grid-connected VSI with an LCL filter. IEEE Transactions on Power Electronics, 28.5: 2259-2268.

[12] Fukuda, S., & Yoda, T. (2001). A novel current-tracking method for active filters based on a sinusoidal internal model. IEEE Trans. Ind. Appl., vol. 37, no. 3, pp. 888–895, May/Jun.

APPENDICES

Appendix A: Mat-lab Code - Steady State Mode

```
% Steady state Mode

t=0:0.0001:0.04;
maxLength=1e4;
t(length(t)+1:maxLength)=0;

Ce=50e-6; % estimated value of capacitor filter
L1e=0.4e-3;   % estimated value of inductor inverter
side filter
L2e=1.2e-3;    % estimated value of inductor grid
side filter
r1e=0.01;         % estimated value of damping
resistor inverter side filter
r2e=0.01;          % estimated value of damping
resistor  grid side filter

Ca=Ce-(15/100)*Ce;    % actual value of capacitor
filter
L1a=L1e-(15/100)*L1e;   % actual value of inductor
inverter side filter
L2a=L2e-(15/100)*L2e;     % actual value of inductor
grid side filter
r1a=r1e-(15/100)*r1e;     % actual value of damping
resistor inverter side filter
r2a=r2e-(15/100)*r2e;% actual value of damping
resistor  grid side filter
dC=Ce-Ca;
dL1=L1e-L1a;
dL2=L2e-L2a;
dr1=r1e-r1a;
dr2=r2e-r2a;
V1g=311; V3g=0; V5g=0;
I2=35;
f0=50;
w0=2*pi*f0;
a1=1;
a2=2;
a3=40;
ki=5e4;
kr=100;
% Reference Grid current
I2ref=(I2/(2*1i))*(exp(1i*w0*t)-exp(-1i*w0*t));
% same length
I2ref(length(I2ref)+1:maxLength)=0;
```

```
% Reference Grid Voltage Vg
Vgf=(V1g/(2*1i))*(exp(1i*w0*t)-exp(-1i*w0*t));
Vg3h=(V3g/(2*1i))*(exp(1i*3*w0*t)-exp(-1i*3*w0*t));
Vg5h=(V5g/(2*1i))*(exp(1i*5*w0*t)-exp(-1i*5*w0*t));
% Then dVg
Vg=Vg3h+Vg5h;

%derivatives
dVgf=(V1g/2)*w0*(exp(1i*w0*t)+exp(-1i*w0*3*t));
dV3gh=(V3g/2)*3*w0*(exp(1i*w0*3*t)+exp(-1i*w0*3*t));
dVg5h=(V5g/2)*5*w0*(exp(1i*w0*5*t)+exp(-1i*w0*5*t));

% Then dVg
dVg=dV3gh+dVg5h;

%same length
Vg(length(Vg)+1:maxLength)=0;
dVg(length(Vg)+1:maxLength)=0;

% Transfer function
k1=Ca*L2a-Ce*L2e;
k2=Ca*r2a-Ce*r2e;
k3=a1*Ca*L2a;
k4=a1*Ca*r2a+a2*L2a;
k5=a1+a2*r2a+a3;
k6=-a1*k1;
k7=-a1*k2+a2*dL2;
k8=a2*dr2;
k9=a1*dC;

w=[w0 3*w0 5*w0 7*w0 9*w0 11*w0 13*w0 15*w0 17*w0 19*w0
21*w0];
s=tf('s');
  for n=1:2:21
R(:,n)=(s/((s)^2+(n*w0)^2));
  end
G=R(1)+R(2)+R(3)+R(4)+R(5)+R(6)+R(7)+R(8)+R(9)+R(10)+R(11);

for r=1:11
N(:,r)= 11* (1i*w(r))^21 + 1.748e09* (1i*w(r))^19 + 1.15e17*
(1i*w(r))^17 + 4.085e24 *(1i*w(r))^15 + 8.543e31*(1i*w(r))^13
+ 1.08e39* (1i*w(r))^11 + 8.162e45* (1i*w(r))^9 + 3.519e52
*(1i*w(r))^7 + 7.877e58 *(1i*w(r))^5 + 7.59e64 *(1i*w(r))^3 +
2.008e70 *(1i*w(r));

D(:,r)=(1i*w(r))^22 + 1.748e08 *(1i*w(r))^20 + 1.278e16
*(1i*w(r))^18 + 5.106e23 *(1i*w(r))^16 + 1.22e31
*(1i*w(r))^14 + 1.8e38*(1i*w(r))^12 + 1.632e45* (1i*w(r))^10
+ 8.798e51* (1i*w(r))^8 + 2.626e58* (1i*w(r))^6+ 3.795e64
*(1i*w(r))^4 + 2.008e70* s^2 + 1.636e75;

end
```

```
T=[N(1)/D(1) N(2)/D(2) N(3)/D(3) N(4)/D(4) N(5)/D(5)
N(6)/D(6) N(7)/D(7) N(8)/D(8) N(9)/D(9) N(10)/D(10)
N(11)/D(11)];

% to get total harmonic distortion
r=1;
X31=((1i*w(r))^2*I2ref*k6+k7*1i*w(r)*I2ref+k8*I2ref+k9*1i*w(r
)*Vg)/(k3*(1i*w(r))^2+k4*1i*w(r)+k5+(ki/(1i*w(r)+kr*T(1))));

r=2;
X3h3=((1i*w(r))^2*I2ref*k6+k7*1i*w(r)*I2ref+k8*I2ref+k9*1i*w(
r)*Vg)/(k3*(1i*w(r))^2+k4*1i*w(r)+k5+(ki/(1i*w(r)+kr*T(2))));

r=3;
X3h5=((1i*w(r))^2*I2ref*k6+k7*1i*w(r)*I2ref+k8*I2ref+k9*1i*w(
r)*Vg)/(k3*(1i*w(r))^2+k4*1i*w(r)+k5+(ki/(1i*w(r)+kr*T(3))));

r=4;
X3h7=((1i*w(r))^2*I2ref*k6+k7*1i*w(r)*I2ref+k8*I2ref+k9*1i*w(
r)*Vg)/(k3*(1i*w(r))^2+k4*1i*w(r)+k5+(ki/(1i*w(r)+kr*T(4))));

r=5;
X3h9=((1i*w(r))^2*I2ref*k6+k7*1i*w(r)*I2ref+k8*I2ref+k9*1i*w(
r)*Vg)/(k3*(1i*w(r))^2+k4*1i*w(r)+k5+(ki/(1i*w(r)+kr*T(5))));

r=6;
X3h11=((1i*w(r))^2*I2ref*k6+k7*1i*w(r)*I2ref+k8*I2ref+k9*1i*w
(r)*Vg)/(k3*(1i*w(r))^2+k4*1i*w(r)+k5+(ki/(1i*w(r)+kr*T(6))))
;

r=7;
X3h13=((1i*w(r))^2*I2ref*k6+k7*1i*w(r)*I2ref+k8*I2ref+k9*1i*w
(r)*Vg)/(k3*(1i*w(r))^2+k4*1i*w(r)+k5+(ki/(1i*w(r)+kr*T(7))))
;

r=8;
X3h15=((1i*w(r))^2*I2ref*k6+k7*1i*w(r)*I2ref+k8*I2ref+k9*1i*w
(r)*Vg)/(k3*(1i*w(r))^2+k4*1i*w(r)+k5+(ki/(1i*w(r)+kr*T(8))))
;

r=9;
X3h17=((1i*w(r))^2*I2ref*k6+k7*1i*w(r)*I2ref+k8*I2ref+k9*1i*w
(r)*Vg)/(k3*(1i*w(r))^2+k4*1i*w(r)+k5+(ki/(1i*w(r)+kr*T(9))))
;
r=10;
X3h19=((1i*w(r))^2*I2ref*k6+k7*1i*w(r)*I2ref+k8*I2ref+k9*1i*w
(r)*Vg)/(k3*(1i*w(r))^2+k4*1i*w(r)+k5+(ki/(1i*w(r)+kr*T(10)))
);
```

```
r=11;
X3h21=((1i*w(r))^2*I2ref*k6+k7*1i*w(r)*I2ref+k8
*I2ref+k9*1i*w(r)*Vg)/(k3*(1i*w(r))^2+k4*1i*w(r
)+k5+(ki/(1i*w(r)+kr*T(11))));

% magnitude of grid current error at
fundamental frequency

harmonicorder=[1 3 5 7 9 11 13 15 17 19 21];
error=((X31)+(X3h3)+ (X3h5) +(X3h7) +(X3h9)
+(X3h11)+(X3h13)+(X3h15)+(X3h17)+(X3h19)+(X3h21
));
figure;
plot(t,error)
```